Hydrological Modelling of Surface Runoff on Brier Island, Nova Scotia

Prepared by

Tim Webster, PhD
Kate Collins, Nathan Crowell, Candace MacDonald, Kevin McGuigan
Applied Geomatics Research Group
NSCC, Middleton, NS
Tel. 902 825 5475
email: tim.webster@nscc.ca

Submitted to

Craig Smith, Nova Scotia Program Manager
Nature Conservancy of Canada
7071 Bayer's Road, Suite 337
Halifax, NS
craig.smith@natureconservancy.ca

February 12, 2015

How to cite this work and report:

Webster, T., Collins, K., Crowell, N., MacDonald, C, McGuigan, K. 2015. Hydrological Modelling of Surface Runoff on Brier Island, Nova Scotia. Technical report, Applied Geomatics Research Group, NSCC Middleton, NS.

Table of Contents

List of Figures

List of Tables

1 Introduction

Brier Island is a small island in the Bay of Fundy, located at the westernmost tip of Nova Scotia in Digby County (Figure 1.1). It has a predominantly rocky coastline defined by basalt bedrock outcrops, and only a small portion of eastern coastline is developed. The island’s southern interior is defined largely by an inland bog, named Big Meadow Bog, which drains northeast into Grand Passage and southwest into one of two barrachois on Brier Island. The barrachois are ponds that are partially separated from the open Bay of Fundy by barrier beaches.

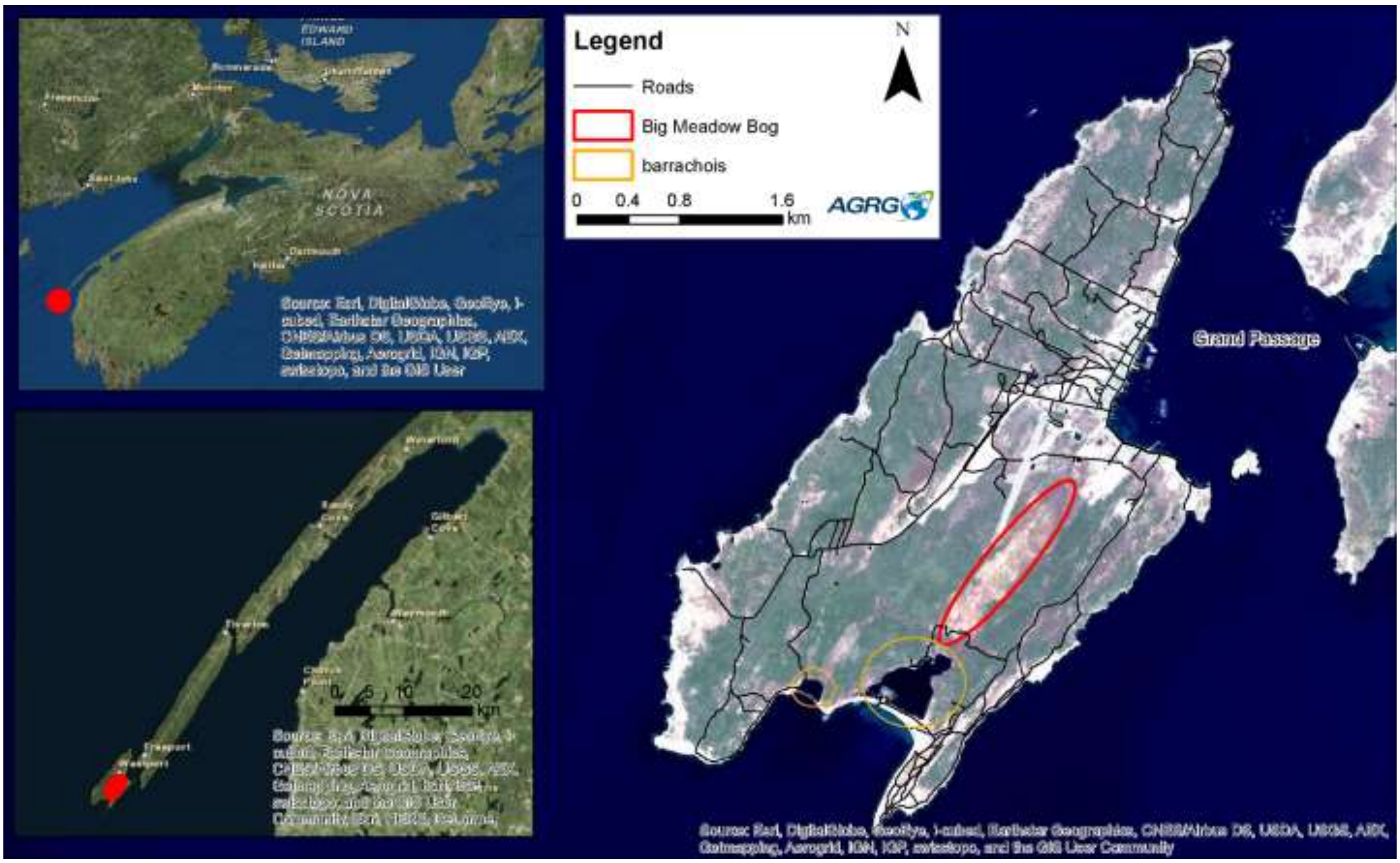

Figure 1.1: Brier Island, Nova Scotia showing Big Meadow Bog, and the barrachois at the southern end of the island.

The hydrology of Big Meadow Bog is important for ecological purposes, as it is home to a rare flower called Eastern Mountain Avens. Attempts made in the past to drain the bog to create more tenable land have disrupted the natural biodiversity of the bog by allowing non-native plant species to flourish, threatening the habitat of the endangered Eastern Mountain Avens (MacDonald and Webster, 2015). This study builds on a preliminary hydrological analysis of the bog completed at the Applied Geomatics Research Group (AGRG) in 2014 (MacDonald and Webster, 2014). Here, we develop a one dimensional (1-D) hydrodynamic model of the bog to understand how water flows within the bog, so that the Nature Conservancy of Canada may use it in their investigation of how the bog would respond to efforts to restore it to a more natural state.

This report first outlines fieldwork and instrumentation (), and then describes the development of the model (). Results are presented and discussed (Section 3). Appendix with weather plots.

2 Methods

Hydrological and hydrodynamic model development and within Big Meadow Bog on Brier Island has required the deployment of multiple field instruments and several field surveys. A high resolution surface and elevation model for Brier Island was developed using lidar data, a remote sensing method using a laser ranging system on an aircraft to survey high resolution topography. This section summarizes fieldwork instrumentation, presents field data, describes the lidar dataset, and outlines the development of the hydrodynamic model.

2.1 Field Work

2.1.1 Instrumentation

Pressure sensors were deployed at three locations in Big Meadow Bog on April 29 and 30, 2014 (Figure 2.1 through Figure 2.4). The locations were chosen in consultation with the Nature Conservancy Canada (NCC) to measure flow in a natural bog drainage feature (NE-DF) and a man-made drainage ditch (NC-DD and SC-DD). At each visit to the study area several measurements were taken, including flow measurements, Real Time Kinematic (RTK) GPS, and photographs (Table 2.2). Flow measurements involve measuring cross-sections of the stream; at every visit to the sensors measurements of water above the sensor were taken to use in validating the pressure sensor data and in building the rating curve. This information was critical to calibrate and validate a hydrologic model for the system, and is discussed in detail in Section 2.3 on the hydrodynamic model.

Please note that the pressure sensors were renamed during the final stages of the writing of this report. Due to the near-complete stage of this report, the original naming scheme has been maintained, but in the future the following terms will be used:

Names used in this report		Name to be used in future reports
Sensor 1	NE-DF	SW-01
Sensor 2	NC-DD	SW-02
Sensor 3	SC-DD	SW-03

Table 2.1: Present and future pressure sensor naming schemes.

Location	Date	Measurements			Notes
		Flow	RTK	Photos	
NE-DF	04/29/2014	x	x	x	Pressure sensor installed at 18:54 GMT. Depth ~ 0.30 m deep, varying over distance. Substrate highly variable. Max flow 0.046 m/s.
	06/19/2014	x	x		Flow measurements taken at 16:34 GMT. Depth ~ 0.40 m deep. Very loose sediment. Max flow 0.102 m/s in middle of channel.
	07/17/2014	x	x		Flow measurements taken at 16:10 GMT. Max depth ~ 0.49 m deep. Incredibly soft muddy bottom. Max flow 0.219 m/s near middle of channel.
	08/11/2014	x			Flow measurements taken at 18:05 GMT. Max depth ~ 0.35 m. Max flow 0.016 m/s in middle.
	12/02/2014			X	Pressure sensor retrieved at 15:00 GMT. ~0.4 m deep, substrate loose and variable.
NC-DD	04/29/2014	x	x	x	Pressure sensor installed at 20:15 GMT. Depth ~ 0.30 m deep, very steep sided. Peat bottom. Max flow 0.032 m/s.
	06/19/2014	x	x		Flow measurements taken at 16:59 GMT. Depth ~ 0.20 m deep. Lightly loose sediment. Max flow 0.027 m/s.
	07/17/2014	x	x		Flow measurements taken at 17:08 UTC. Max depth ~ 0.26 m deep at left bank. Small waterfall upstream of sensor and measurements location. Max flow 0.034 m/s
	08/11/2014	x			Flow measurements taken at 18:40 GMT. Depth and flow fairly uniform ~0.24 m and 0.005 m/s.
	12/02/2014			X	Pressure sensor retrieved at 15:15 GMT. Water depth ~ 0.32 m.
SC-DD	04/30/2014	x	x	x	Pressure sensor installed at 14:08 GMT. Depth ~ 0.20 m deep, varying greatly over distance. Small waterfall, fallen trees, max flow 0.029 m/s.
	06/19/2014	x	x		Flow measurements taken at 18:19 GMT. Depth ~ 0.20 m deep. Very loose sediment. Max flow 0.037 m/s near left bank of channel.
	07/17/2014	x	x		Flow measurements taken at 18:27 UTC. Max depth ~ 0.20 m deep at left bank. Very soft bottom, incredibly overgrown. Max flow 0.049 m/s.
	08/12/2014	x			Flow measurements taken at 13:00 GMT. Channel deepest at left bank (0.15 m) and fastest at right bank (0.023 m/s).
	12/02/2014			X	Pressure sensor retrieved at 16:15 GMT. Depth ~0.20 m, sediment and particulate matter accumulated downstream of sensor mount.

Table 2.2: Pressure sensor fieldwork summary.

Location	Sensor Brand	Data Collection Started	Data Collection Ended	Sampling Interval	Coordinates
NE-DF	Hobo	April 29, 2014 18:54 GMT	December 2, 2014 15:00	15 min	66°21'18.72"W,

					44°15'18.72"N
NC-DD	Hobo	April 29, 2014 20:15 GMT	December 2, 2014 15:15	15 min	66°21'22.32"W, 44°15'17.28"N
SC-DD	Solinst	April 30, 2014 14:08 GMT	December 2, 2014 16:15	15 min	66°22'1.92"W, 44°14'38.04"N

Table 2.3: Pressure Sensor installation and recovery summary.

The hydrological model required precipitation, temperature, and pressure data time series as input variables. The sources of these data are shown in Table 2.4. Two meteorological stations existed on Brier Island prior to the start of this project: and Environment Canada (EC) station located at the northern tip of the island and an AGRG station located near the center of the island (Figure 2.1). Precipitation data is essential to be used as input for the watershed runoff model, and a high frequency sampling interval is critical. The EC station's hourly observations were not appropriate, so the AGRG weather station was modified to include a rain bucket. Air

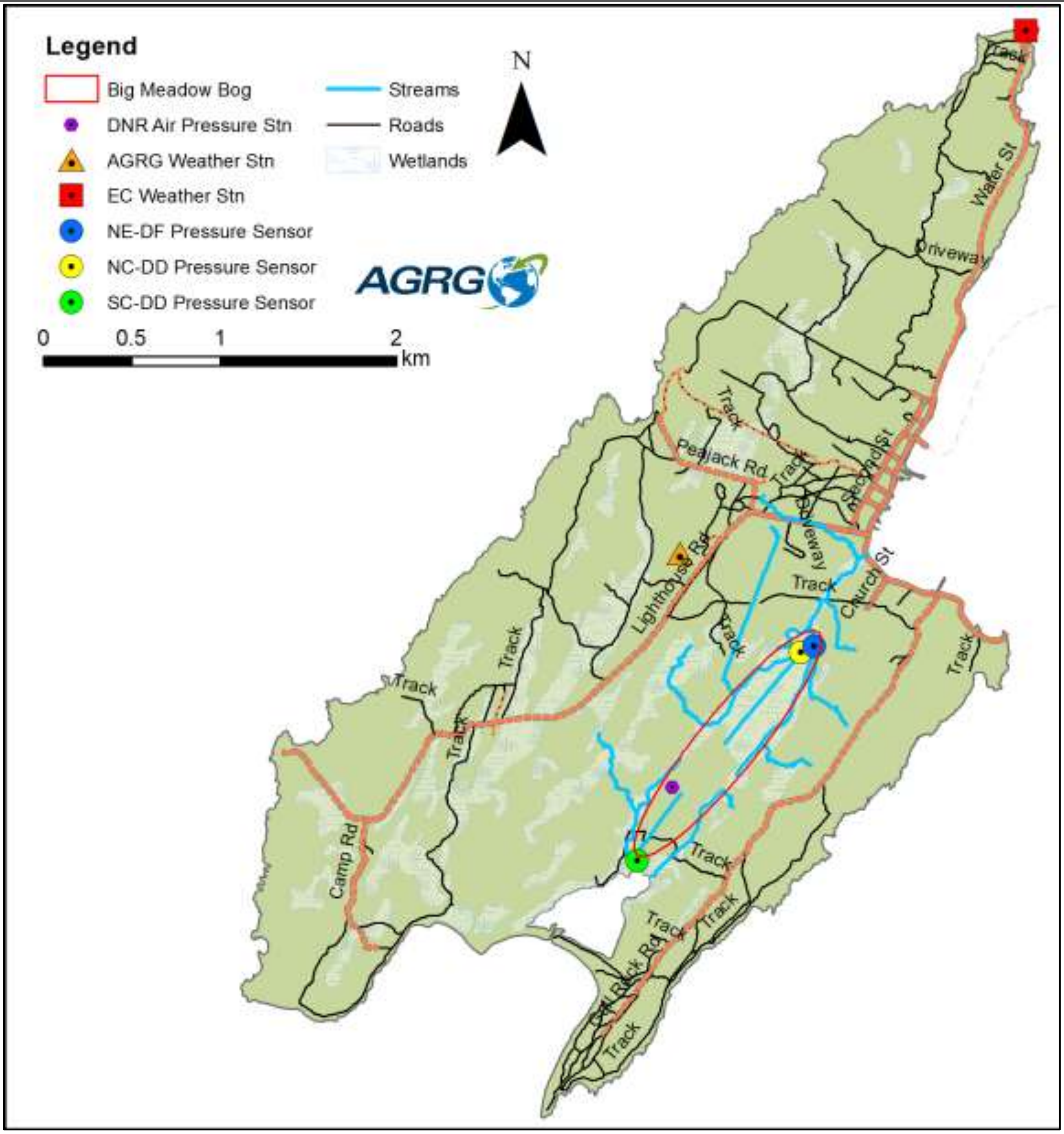

Figure 2.1: Map showing the three pressure sensors and two meteorological stations used for this study.

Data Source	Temperature	Atmospheric Pressure	Precipitation	Sampling frequency	Coordinates
EC	Full record	Full record	Full record	Hourly	66°20'31.2"W, 44°17'13.2"N
AGRG	Full record	None	May 13 – Dec 2, 2014	5 minutes	66º21’54” W, 44º15’36” N
DNR	None	April 30 – Oct 14	None	Hourly	66º21’54” W, 44º14’52” N

Table 2.4: Meteorological data summary. Full record indicates April 29 - Dec 2 2014.

Figure 2.2: NE-DF sensor map and installation photos and notes.

Figure 2.3: NC-DD map and installation photos and notes.

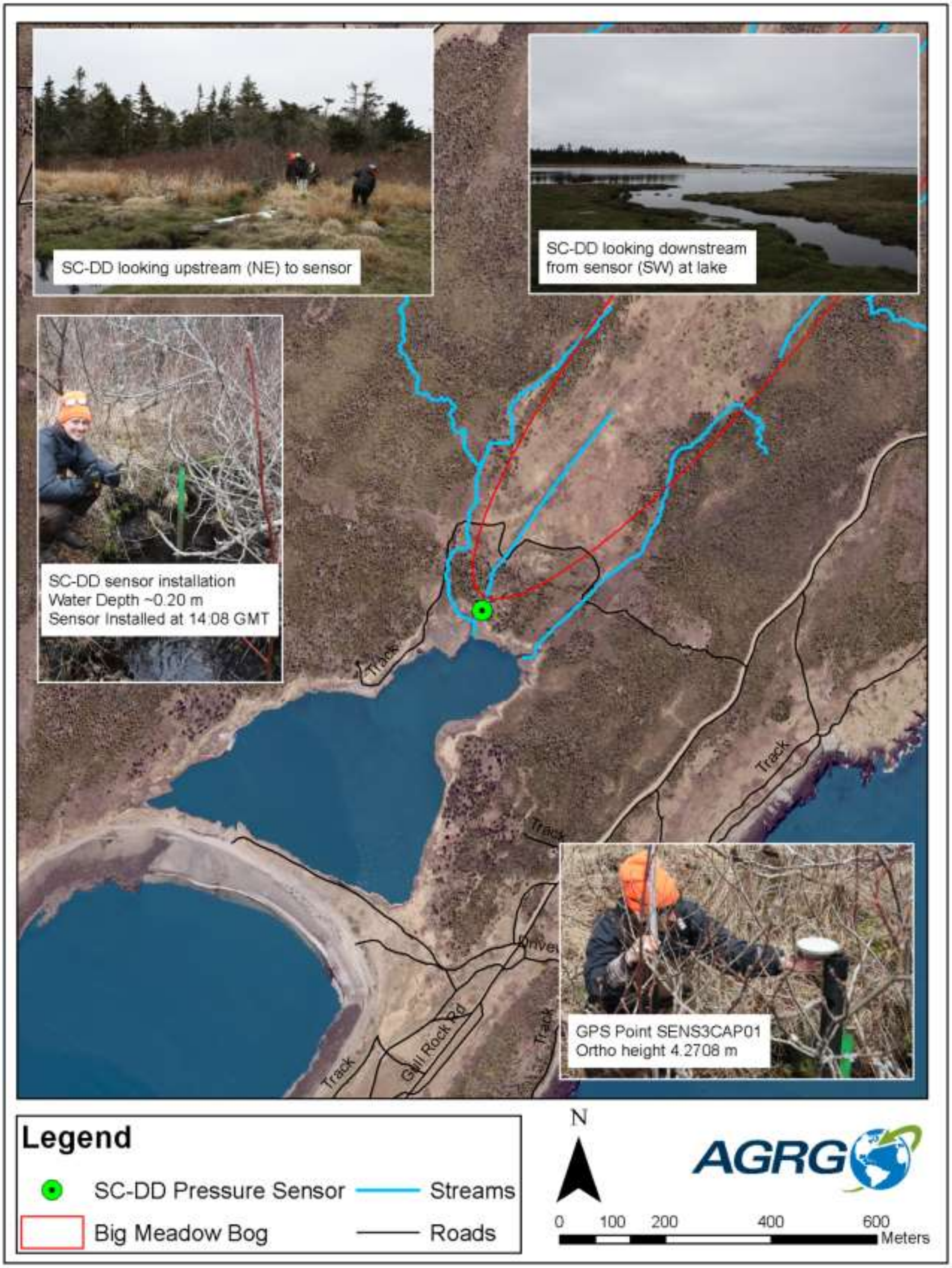

Figure 2.4: SC-DD map and installation photos and notes.

2.1.2 Data

Figure 2.5 shows the water level data from all three pressure sensors for the entire deployment. Precipitation data from the AGRG weather station highlights the coupling of rainfall events and increased water level. Water levels measured during field visits are shown as validation points on the graph. The differences between observed water levels and levels recorded by the pressure sensors are -0.28 cm, -0.12 cm, and 3.3 cm for the NE-DF, NC-DD, and SC-DD locations, respectively. Note that the SC-DD data ends on Oct 14 because the air pressure data obtained from the Department of Natural Resources (DNR) used to compensate the water pressure data ended on that date, and this was the only data suitable for use with the Solinst pressure sensor. The northern sensors (Hobo brand) were compensated using EC air pressure data, which spanned the entire length of the deployment (Table 2.4).

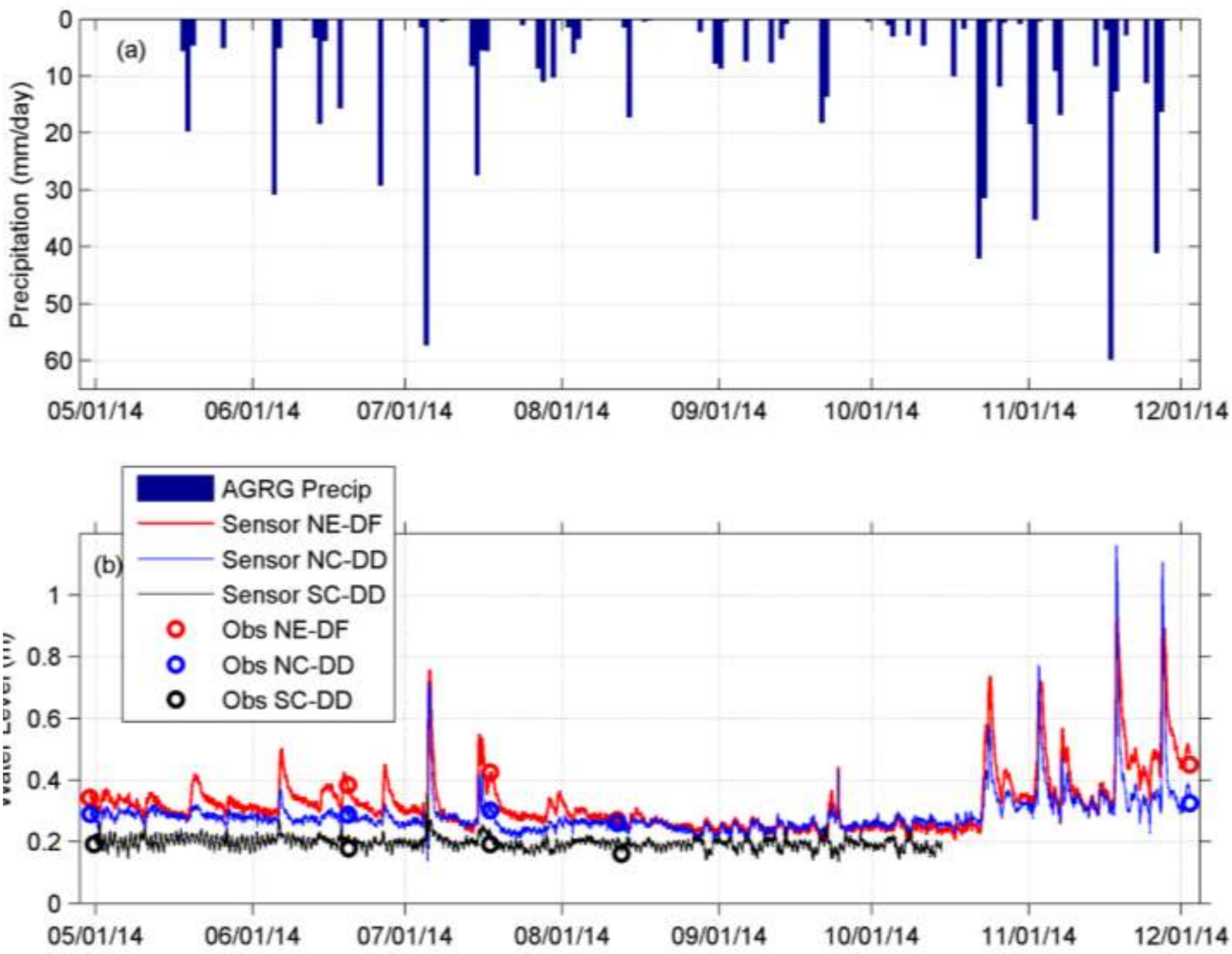

Figure 2.5: (a) Daily precipitation; (b) water level at each of the three sensors as recorded by the sensors, with observed water levels shown as circles.

The time lag between a precipitation event and the peak of an increased water levels are shown for two events at each study location in Figure 2.6 through Figure 2.8. At the northern sites the time lag during the dryer summer period after a large rain event is longer than after a rain event in mid-November, after several rain events. At the southern site, there was often no time lag at all; this could be a factor of the behavior of the water in the ditch and the absence of true overland flow, but the distance between SC-DD and the AGRG weather station is greater for this study location and may also play a role, such that the precipitation arrives at the pressure sensor location before it arrives at the weather station.

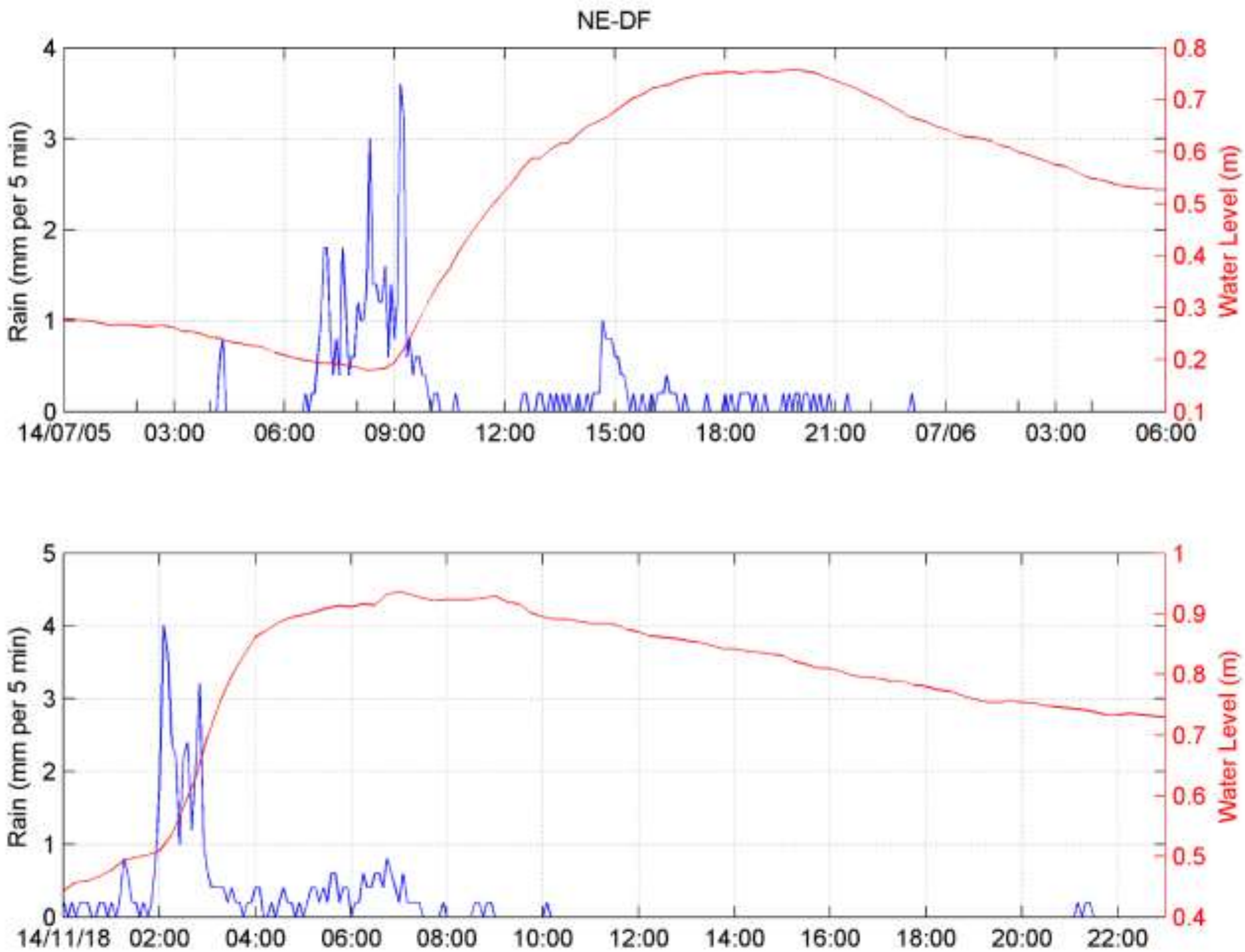

Figure 2.6: Lag at NE-DF between precipitation (as observed at 5 minute sampling interval) and water level on July 5, 2014 (top) and on November 18, 2014. During July when the ground was drier, the lag was ~10-12 hours; in November when the ground was likely much wetter the lag is closer to ~6 hours.

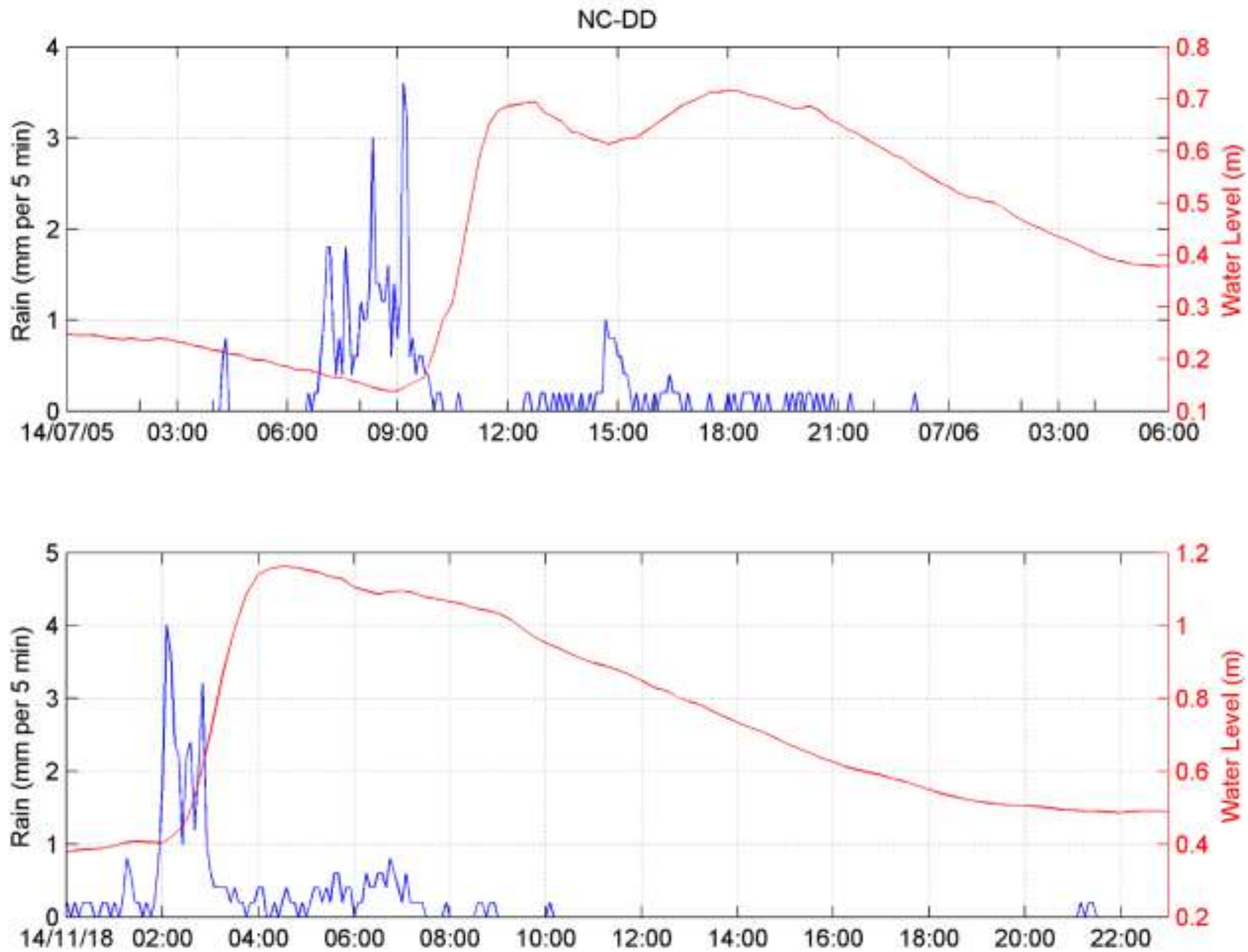

Figure 2.7: Lag at NC-DD between precipitation (as observed at 5 minute sampling interval) and water level on July 5, 2014 (top) and on November 18, 2014. During July when the ground was drier, the lag was ~8-10 hours; in November when the ground was likely much wetter the lag is closer to ~3 hours.

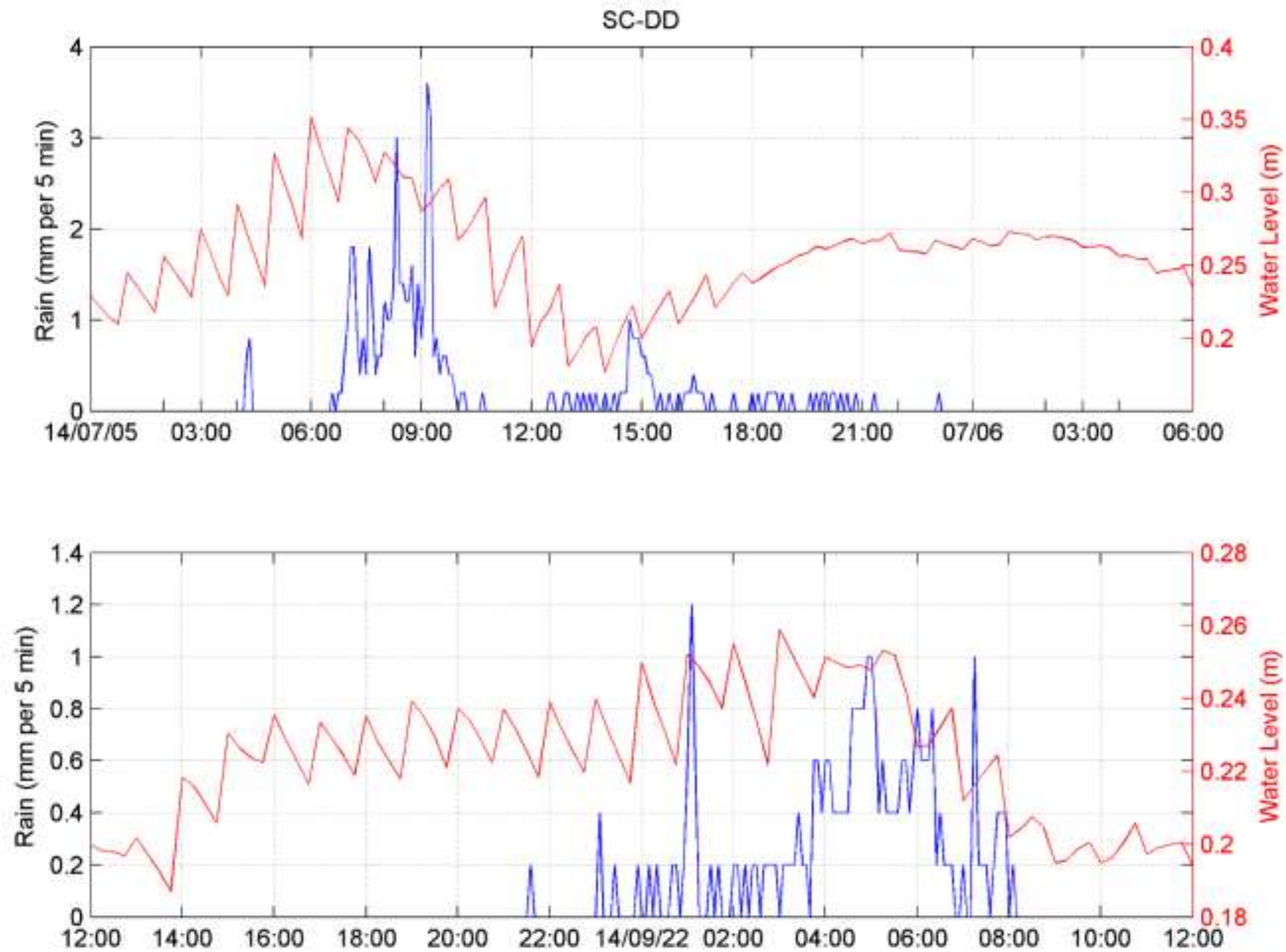

Figure 2.8: Lag at SC-DD between precipitation (as observed at 5 minute sampling interval) and water level on July 5, 2014 (top) and on September 21 and 22, 2014. We see almost no lag during either time frame.

The water level data at the southern site (SC-DD) exhibits frequency peaks at one and two cycles per day. These are likely associated with the diurnal and semi-diurnal components of the tide (Figure 2.9). The drainage ditch SC-DD empties into the barrachois at the southern tip of Brier Island, which is influenced by the large tides of the Bay of Fundy. The amplitude of the signal in the pressure record is almost 20 times smaller than the tides predicted for St Mary's Bay. A more complex study of the tides and their influence on the bog is required, but it appears clear that there is tidal influence at SC-DD, although it is very small.

A potential alternate explanation for the diurnal signal evident in the water level at SC-DD is evapotranspiration. Figure 2.10 shows that the water level increases following the daily temperature maximum, and begins to decrease approximately four hours after the temperature peak. The lag time is likely explained by the time for the transfer of heat between air and water.

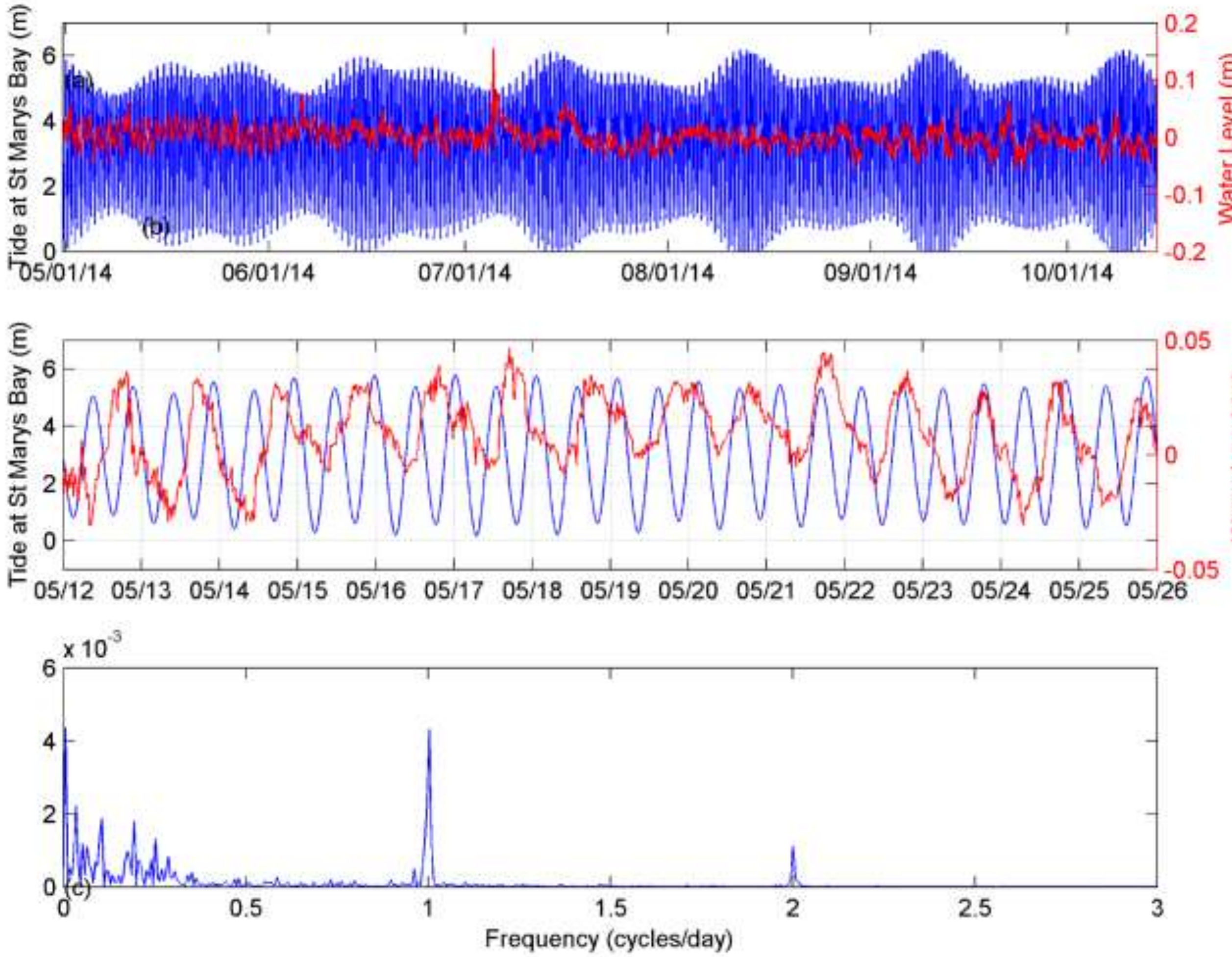

Figure 2.9: Predicted tide at St Mary's Bay, NS, and normalized water level (mean removed) measured by the sensor at SC-DD for (a) the entire deployment and (b) a two-week period; (c) shows a frequency analysis of the normalized water level with peaks at one and two cycles per day.

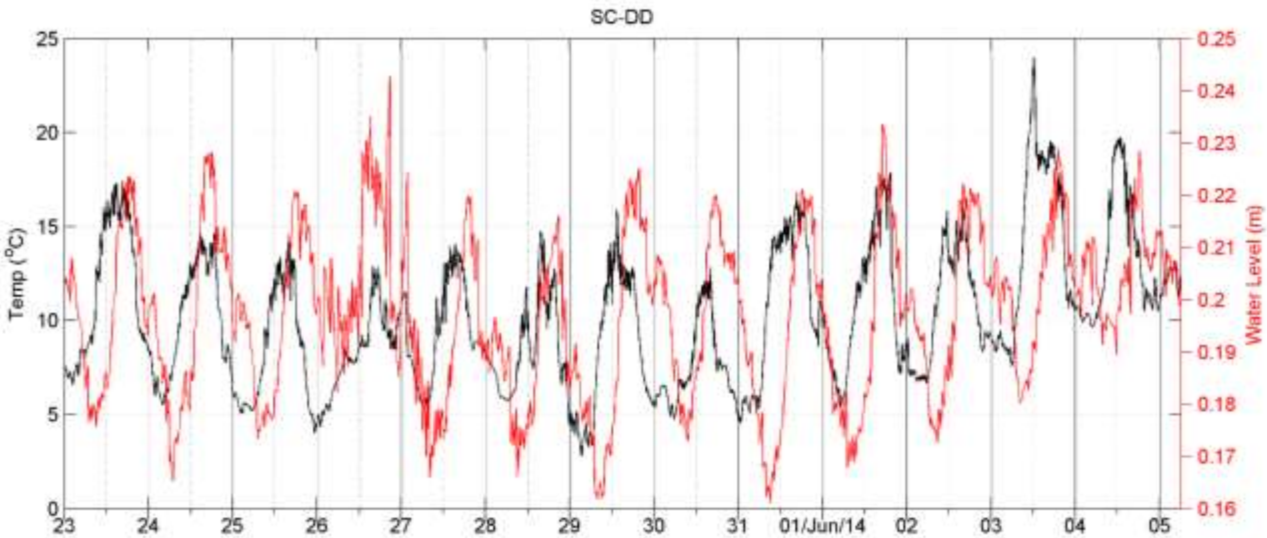

Figure 2.10: Temperature and water level at SC-DD. Water level increases following the daily temperature peak.

Temperature, evapotranspiration, rainfall and air pressure data required for model inputs are shown for the duration of the study in Figure 2.11. The entire meteorological dataset recorded by the AGRG weather station between May and December 2014 is shown in Appendix A: Weather Plots.

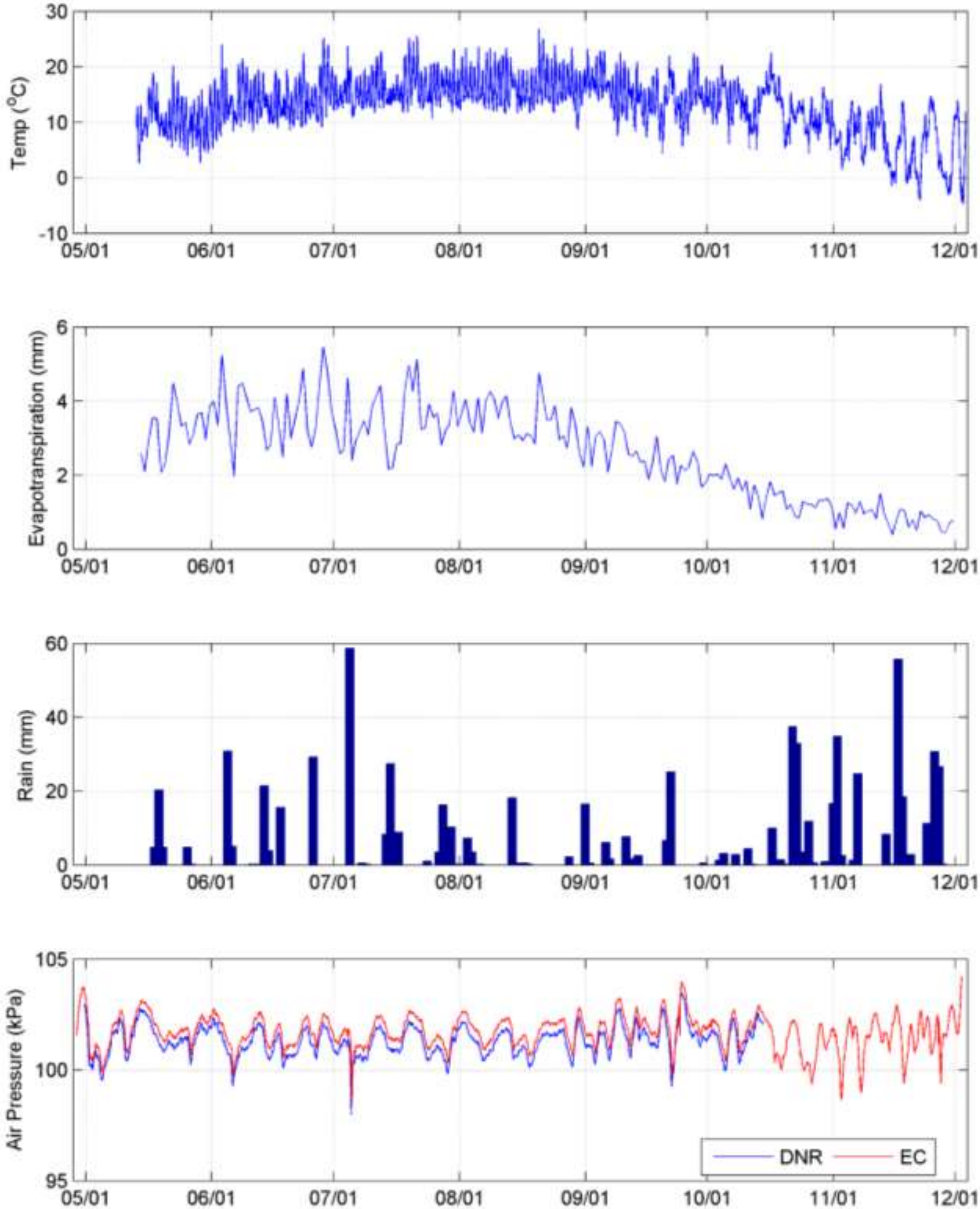

Figure 2.11: Meteorological data used for model input recorded during the study period. Panels from top to bottom show temperature (AGRG), evapotranspiration (derived from AGRG temperature), rain (AGRG), and air pressure (DNR and EC).

2.2 Lidar Data

A lidar survey of Brier Island was conducted by AGRG in October, 2006, and an aerial survey that resulted in orthophoto mosaics was flown in May 2010. Details on both of these datasets, and a validation of the lidar data, are found in MacDonald and Webster (2014). A colour shaded relief map of the data is shown in Figure 2.12.

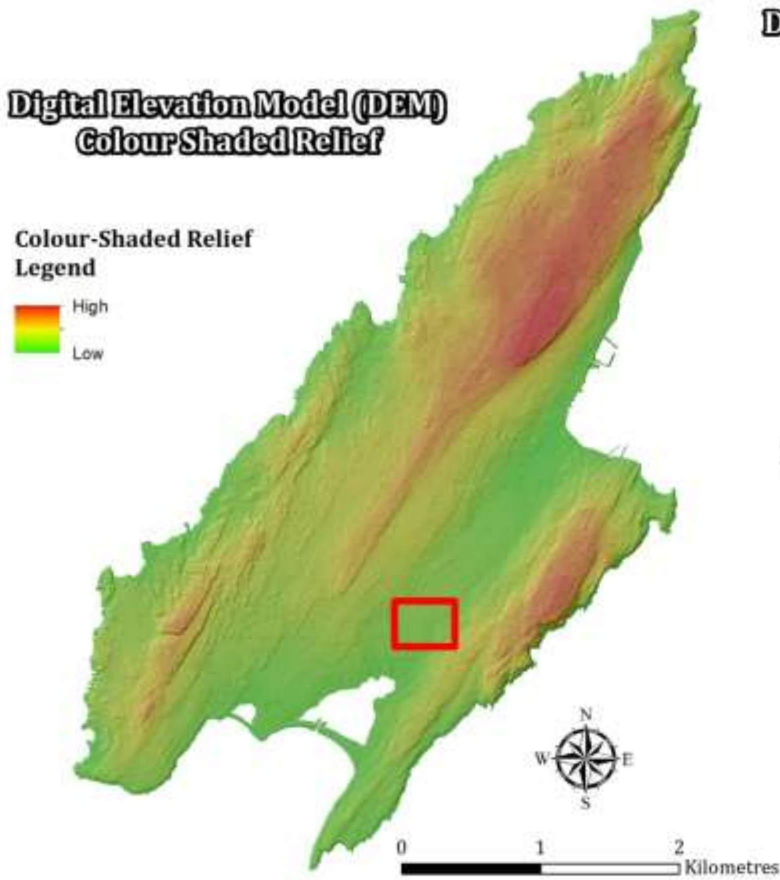

Figure 2.12: Colour shaded relief maps of the 2006 LiDAR derived 1 m digital elevation and surface models of Brier Island from MacDonald and Webster (2014).

2.3 Hydrodynamic Modelling

The Mike 11 software package, developed by DHI, was used to create one-dimensional hydrodynamic models. Simulations were conducted using rainfall and temperature data to drive the model and simulate the water level at the pressure sensors following heavy rainfall events. The rainfall runoff model was validated and calibrated using water depth sensors deployed in the river system, periodic river flow measurements, and high precision RTK GPS river stage measurements collected throughout the project.

2.3.1 DEM preparation

The watershed extents for each drainage system being modelling were calculated using a suite of hydro tools within the ESRI ArcMap 10 software package which relied heavily on elevation data obtained from the 1 m lidar-based DEM. The tools were used to simulate theoretical drainage between adjacent cells based on elevation differences to form watershed boundaries and river networks based on accumulated flow calculations. The DEM was appropriately prepared by lowering elevation values where culverts or bridges existed to ensure proper drainage characteristics between adjacent cells. In the correction process, each structure was removed from the DEM and the lowest surrounding elevation value was used for the gap. The catchments draining into Sensor 1 at the NE-DF encompassed an area of 0.55 km^2, catchments draining into Sensor 2 at the NC-DD encompassed 0.76 km^2 (Figure 2.13), and catchments draining into Sensor 3 at the SC-DD encompassed 0.056 km^2. Catchment areas and land cover drainage characteristics were used as an input parameter within the Mike 11 Rainfall-Runoff model.

The Mike11HD model requires accurate stream and floodplain topography in order to simulate the flow of water through the system. The river network was sectioned into unique branches with length (chainage) measured in meters (Figure 2.13). Each branch was then linked with its appropriate catchment in order to create a stable network input for simulations. Mike 11 HD does not continuously calculate flow along river branches, rather, it calculates flow at defined cross-sections in order to transfer flow between cross-sectional distances where equations are based on the conservation of momentum principle. Cross-sections were manually digitized across river branches and flood plains perpendicular to the direction of flow (Figure 2.14). Cross-sections were roughly spaced at 100 m intervals along river branches while ensuring that a cross-section was drawn at the start and end chainage of each river branch. Cross-section width was dependent on topography and was ensured to capture potential flood plains during significant flooding events. Elevation was extracted from the DEM and applied to each cross-section. Conveyance and water level were calculated for each of the two-dimensional cross-sections based on theoretical water elevation within the cross-section at 1 cm increments. Cross-section topography and conveyance potentials were stored within the final cross-section input file for hydrodynamic (HD) simulations.

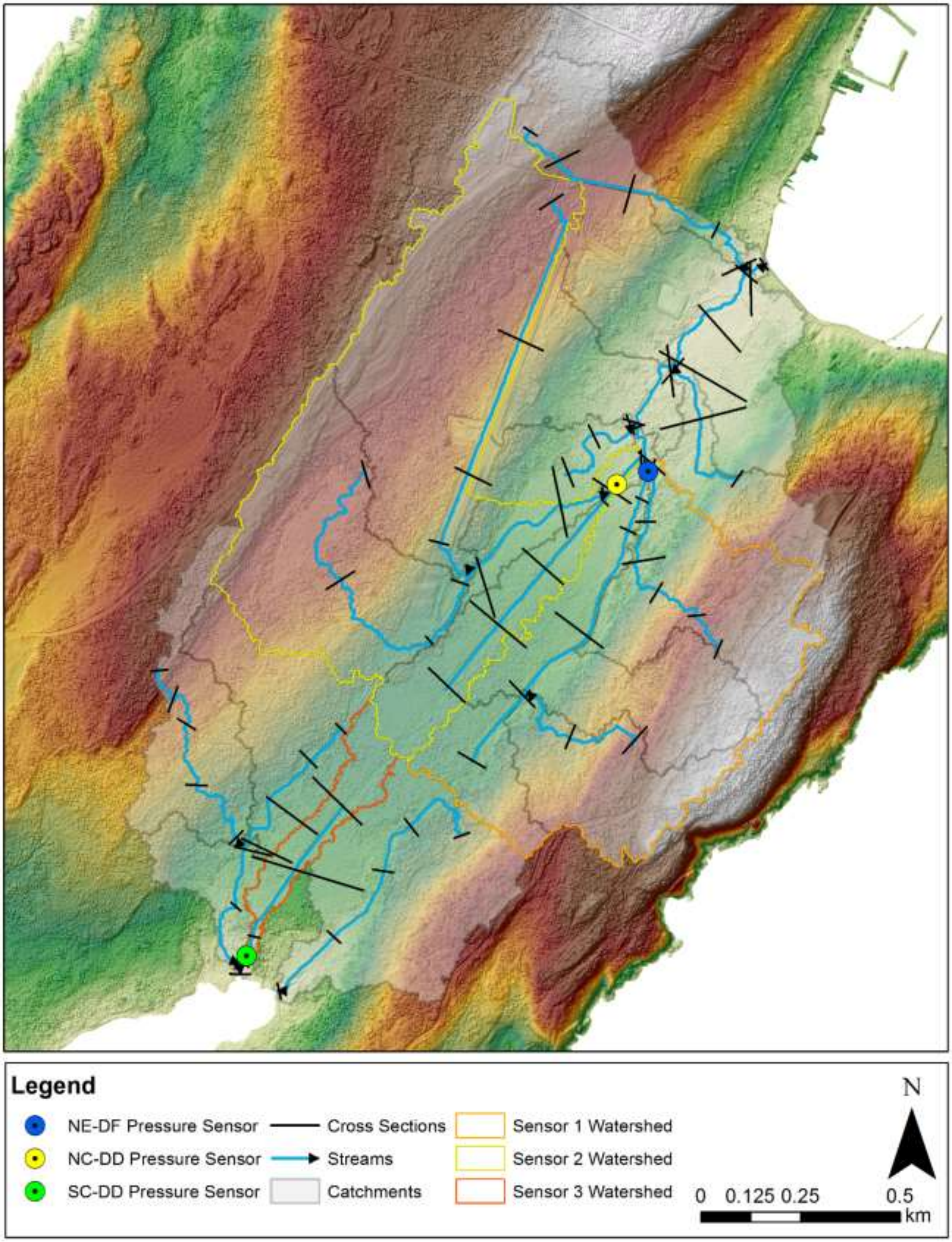

Figure 2.13: Digital elevation model of Brier Island showing the three pressure sensors, watersheds and catchment areas, stream branches and the cross-sections used in the 1-D hydrodynamic model.

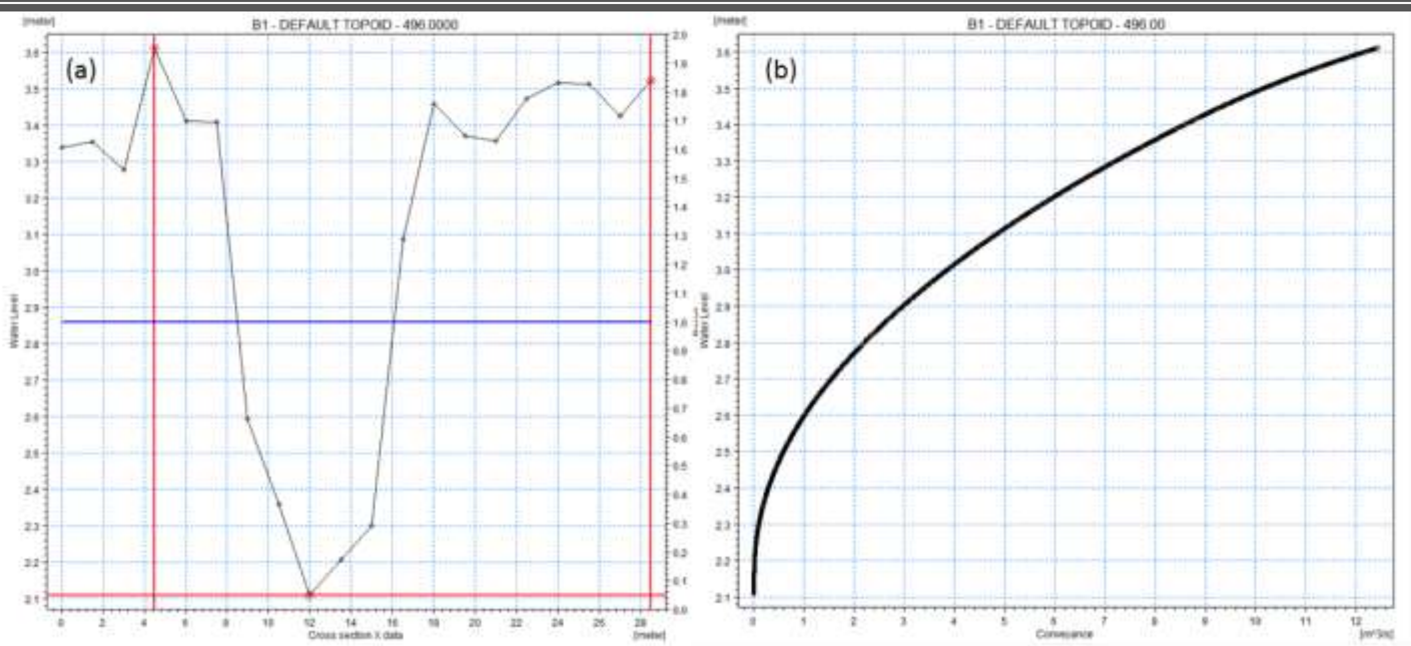

Figure 2.14: (a) Branch B1 cross-section oriented perpendicular to flow. Elevation data along the length of the cross-section were extracted from the DEM. The minimum possible water level corresponded to the minimum elevation within the cross-section (horizontal red bar) and the maximum flood banks of the cross-section were drawn at the left and right end points (vertical red bars); (b) potential conveyance was calculated based on water level increments within the possible flood area.

2.3.2 Rainfall Runoff Model

The Brier Island rainfall runoff model was driven by a Rainfall Dependent Inflow and Infiltration model (RDII) within the Mike11 software suite. The rainfall runoff model is a generalized watershed model that simulates the discharge of water by quantifying routing times and storage zone capacities. The model is forced with observed precipitation and evapotranspiration, a measurement derived from daily temperature minima and maxima indicating the amount of water entering the air from evaporation and plant transpiration, using data from the AGRG Weather Station. The water pressure recorded by the three stage sensors is converted to water depth by measuring the offset between the sensor GPS position and the recorded depth. Variances in barometric pressure are compensated for using readings from the DNR and EC barologgers. Figure 2.1 shows the locations of the sensors, Table 2.4 details the data records, and Figure 2.11 shows the data.

Rating curves were attempted for the three locations in order to relate water level (stage) to discharge. The rating curves use observed flow measurements that were taken using a Valeport electromagnetic (EM) flow meter. Flows were recorded at the sensor locations perpendicular to the river orientation at a 0.2 m sampling interval. Velocity was measured for each of the 0.2 m columns using the average of 30 second sampling intervals which recorded 1 sample per second. Water velocity was measured at the 60% depth (in a water depth of 10 cm, a velocity measurement was recorded at 6 cm). Velocity was averaged over each of the 0.2 m columns to produce an average flow measurement. Total discharge was calculated by summing flows from each of the 0.2 m columns. Water level measurements were measured during each visit to the site; the difference between levels measured by the pressure sensor and the measured levels were minimal. The rating curves and equations for each location are shown in Figure 2.15. The discharge rating curve was a best fit line to the observed river flow and stage data. However, it is clear that the rating curves were unsuccessful at the NC-DD and SC-DD locations, and minimally successful at the NE-DF location. Reasons for the poor rating curves are discussed more in Section 3 and relate to the way that water flows within a bog compared to a more typical river.

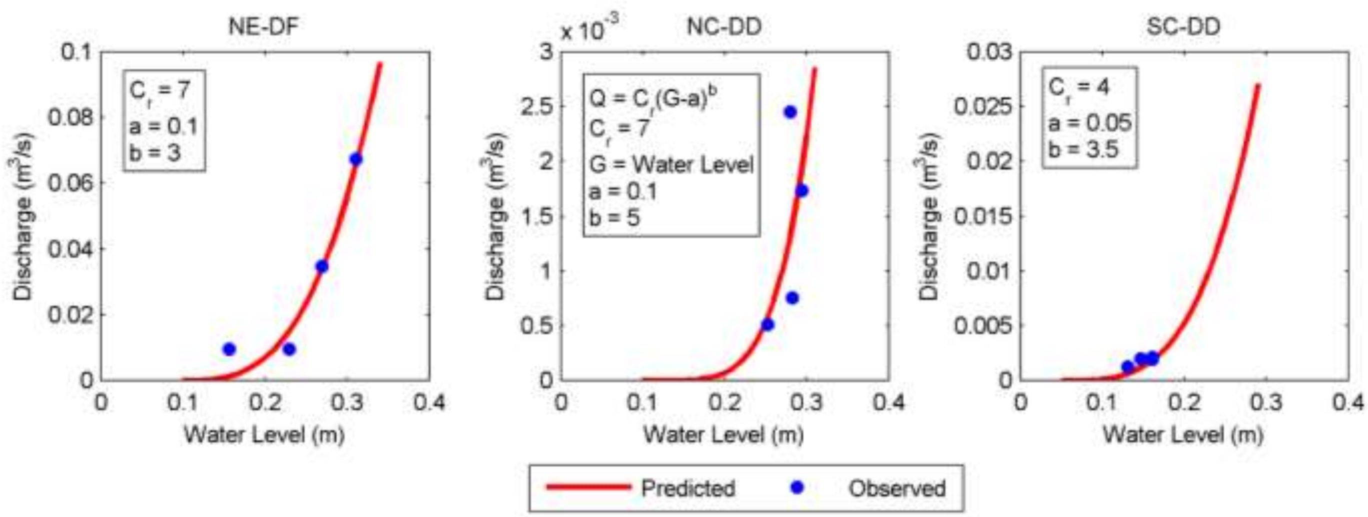

Figure 2.15: Rating curves derived from measured water level and discharge at each sensor. Note the different scale of the y-axis in each panel showing the differences in discharge at each location.

If the rating curves had been successful, the equation for discharge resulting from the rating curve would have allowed us to use the continuous water level stage data recorded by the sensors to produce a time series of discharge at each location, which are used as model calibration and validation for the Rainfall-Runoff model. The Rainfall Runoff models for each sensor would then have been calibrated using an iterative process of fine-tuning watershed infiltration/runoff parameters until the modelled discharge matched the observed. Since we did not trust the rating curves, we were not able to calibrate the River Runoff model before integrating it with the 1-D hydrodynamic model. The NAM parameters were instead fine-tuned by matching observed water levels against simulated 1-D hydrodynamic model water levels to calibrate and validate model results. This process is described in the next section.

2.3.3 1-D Hydrodynamic Model

One dimensional hydrodynamics were modeled using the Mike11HD component of the Mike software suite by DHI. The hydrodynamic model component required Rainfall Runoff models for each sub-catchment in the each of the three watersheds and suitable river cross-sections for conveyance calculations and floodplain delineation, as described earlier. Typically, the calibrated rainfall runoff model would be used to provide the hydrodynamic model with inflow data after rainfall events. Since we did not trust the rating curves, we calibrated the River Runoff model and the 1-D HD model simultaneously using water level measured at the pressure sensors for observations. Inflow from catchments is routed to the appropriate river branches by the hydrodynamic model and flow is simulated to the downstream terminus of each river network. The hydrodynamic water levels were calibrated against observed water level records for the month of July to ensure that flow was being properly routed between cross-sections and that bed resistance values were realistic (Figure 2.16). Model simulations for the fall (Figure 2.17) show that the calibration to the July precipitation events was well done, as the modelled and observed water level in November agree nicely at Sensors 1 and 2 (NE-DF and NC-DD). The the entire study period is presented in Appendix B, Figure 7.1, and shows a decrease in base flow, most markedly at Sensor 3 (SC-DD) that is discussed in the Discussion section.

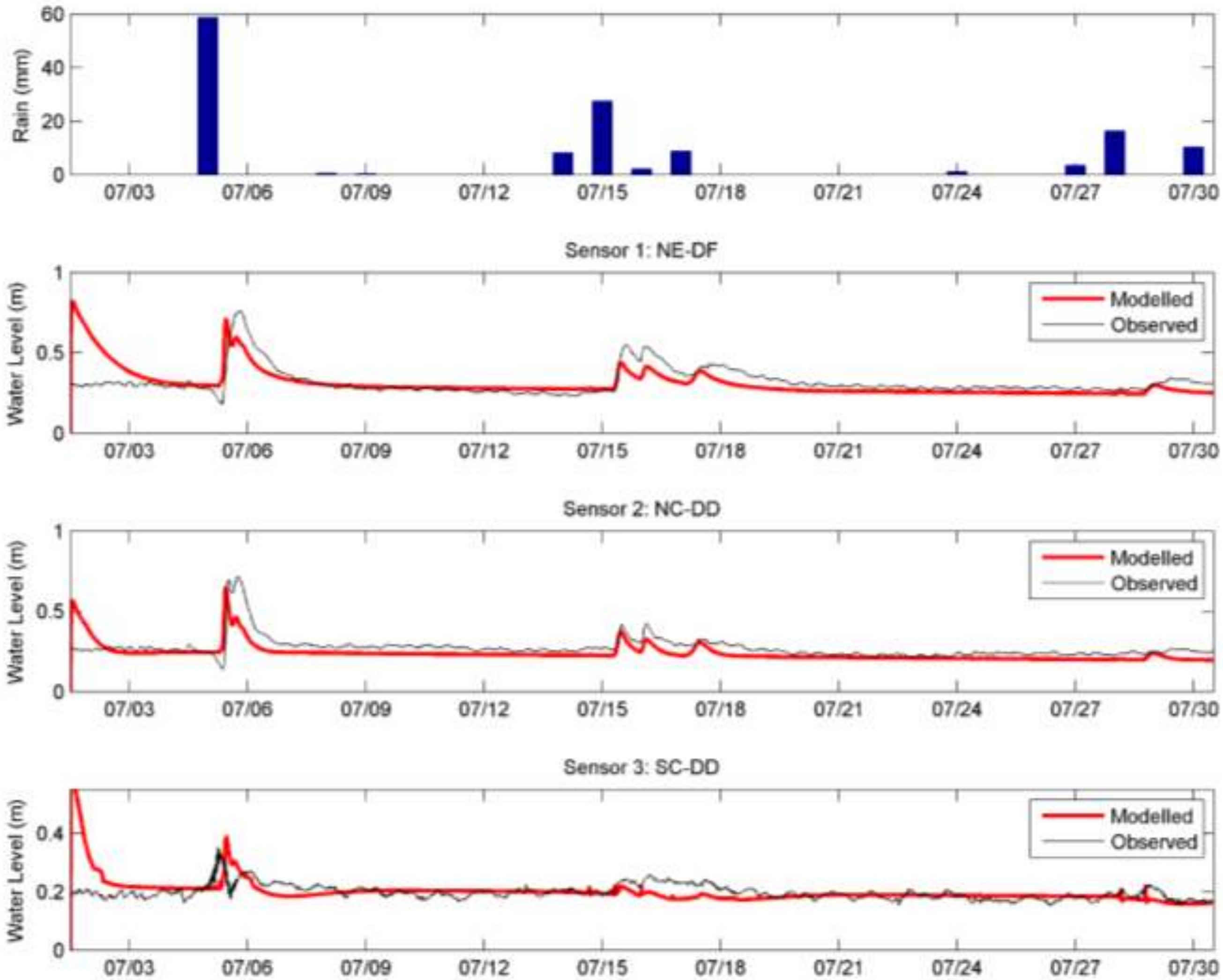

Figure 2.16: Precipitation (top); modelled and observed water level at each sensor location during July 2014.

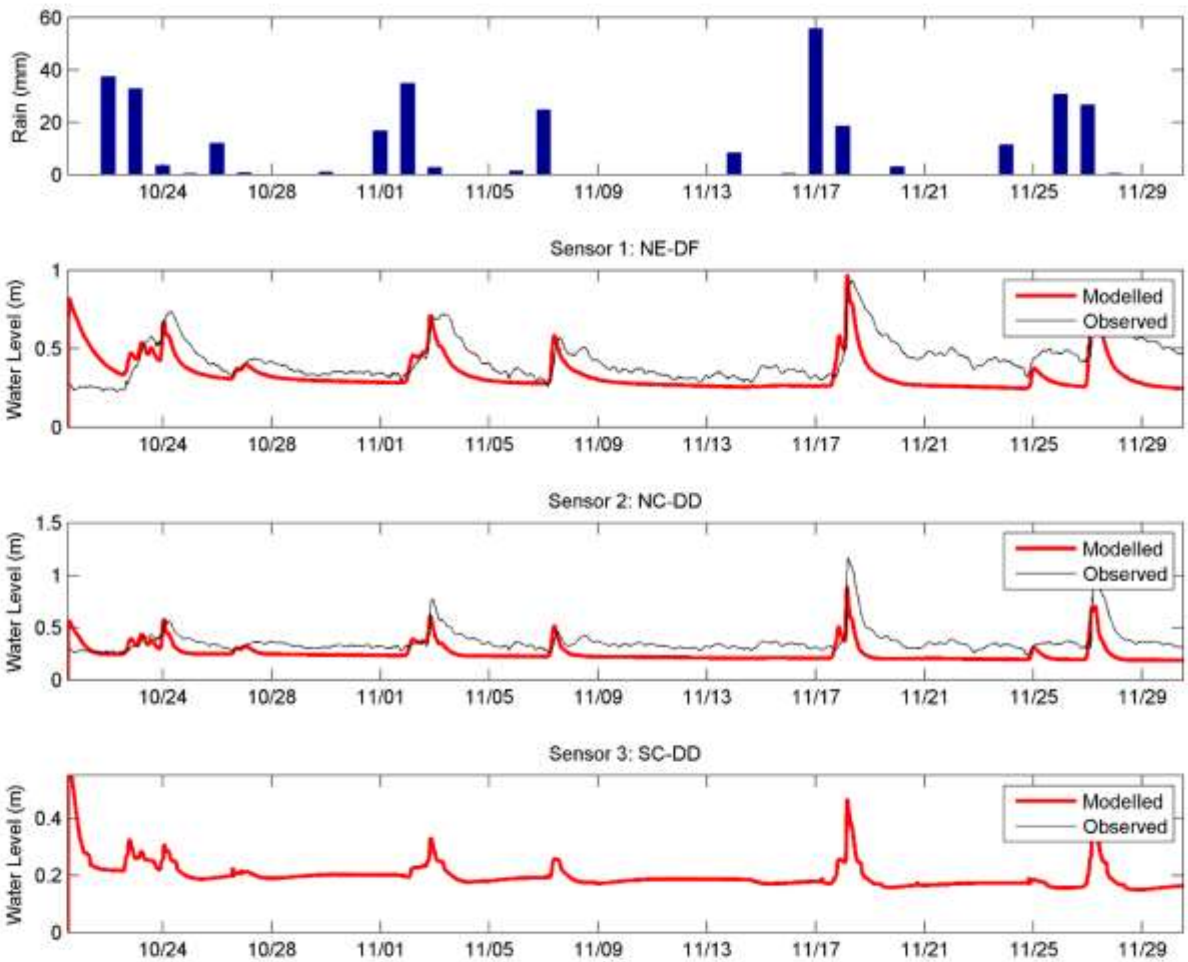

Figure 2.17: Water level calibration plot for October 20 – Nov. 30, 2014.

The calibrated Rainfall Runoff model was then used to model discharge (Figure 2.18). Since no discharge time series' were generated from the pressure sensor data using rating curves, modelled discharge is plotted alongside observed water level. Discharge is greatest at NC-DD and smallest at SC-DD. At all three locations, agreement between precipitation events, and discharge and water level response, are good, although less so at the southern location where peaks in water level are less evident. Agreement between observed (blue circles) and modelled discharge are also inconsistent between the sensors, with the northern sensors agreeing well but at the southern sensor the modelled base flow is higher than the observed low flow.

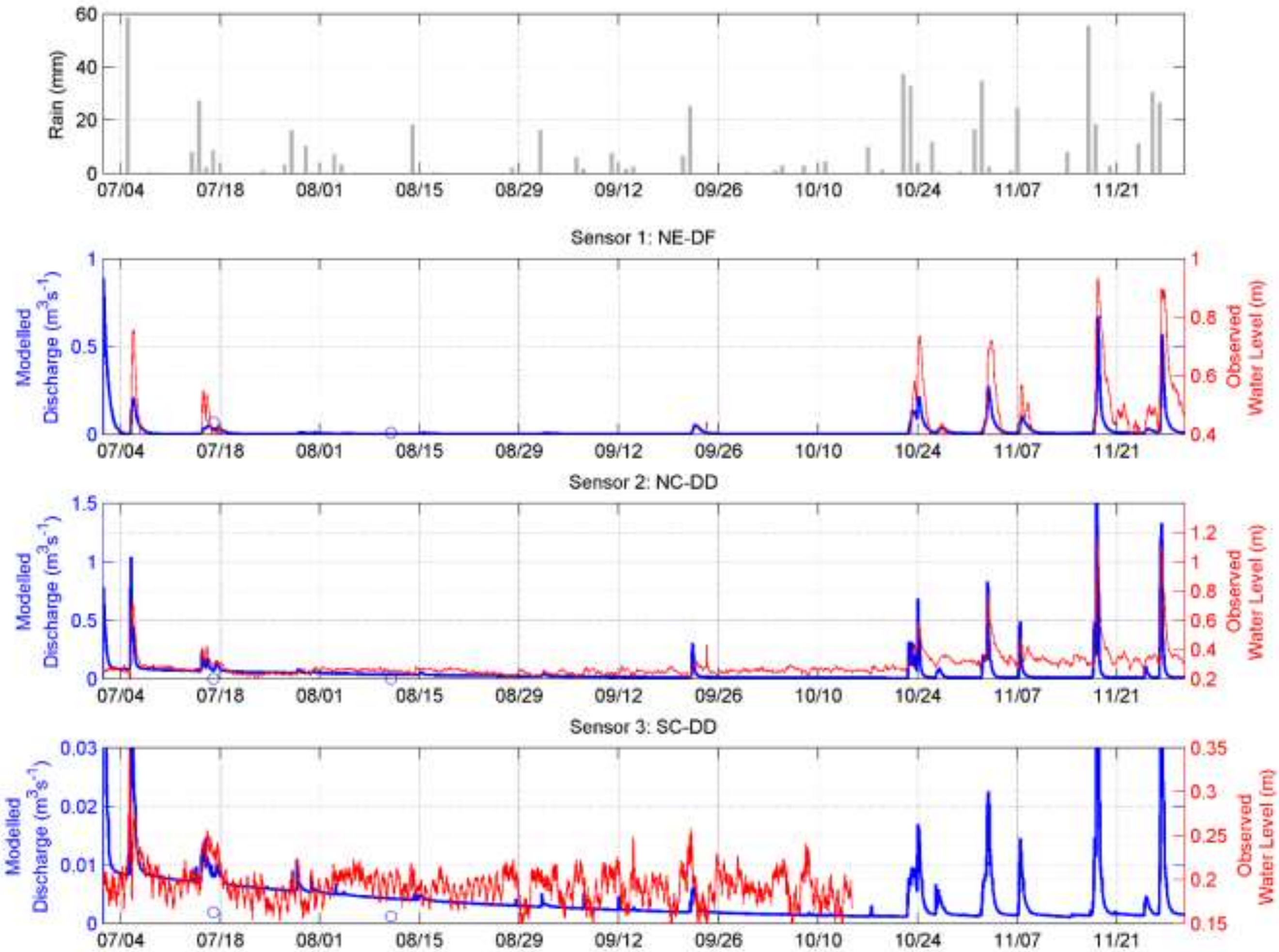

Figure 2.18 Precipitation (top panel); modelled discharge (left axis, blue) and observed water level (right axis, red) between July 1 and Nov 30. Blue circles denote field observations of discharge. Note the different y-axis scales for each subplot.

3 Results and Discussion

3.1 Overland Flow, Inter Flow, and Base Flow

In order to restore Big Meadow Bog to its natural state by eliminating the central drainage ditch, a good understanding of how water is flowing within the bog is essential. The Mike11 1-D model breaks down the modelled runoff into overland flow, inter flow, and base flow for each catchment. The modelled baseflow represents groundwater flowing into the streams, and is present during times of low flow such as dry seasons. Overland flow represents the runoff to the streams during precipitation events, and interflow is a transition between overland and base flow (DHI, 1999). When we use the Mike 11 1-D model, the baseflow values are determined during the calibration process.

The total runoff per catchment is the sum of overland, inter, and base flow. The total runoff per watershed is the sum of total runoff per catchment within each watershed. Labelled catchments and watersheds are shown in Figure 3.1. The sensor at the NE-DF location is representing the flow from five catchments that make up its watershed: C5C1, C5C2, C6C1, C6C2, and C7C1; the largest is C6C1 and the smallest is C5C1. The sensor at the NC-DD location represents the flow from five catchments on the western side of the bog: C1C5, C1C6, C8C1, C8C2, and C9C1; C9C1 is the largest and C1C5 is the smallest. The artificial drainage ditch is contained in both C1C5 and C1C6. The southern watershed contains only one catchment, B1C2, the artificial drainage ditch.

There are two other streams entering the barrachois at the southern extent of the island, but they drain areas outside the bog and do not pass through the sensor at SC-DD. This means that any modelling we could have done on these streams would have been based on the assumptions that the streams behave in the same manner as the modelled stream at SC-DD, and modelled water level of those streams would have been validated using the SC-DD pressure sensor data, another assumption. Therefore, the only modelled stream is the drainage ditch flowing into the pressure sensor at SC-DD and draining catchment B1C2. Similarly, streams outside the watersheds of Sensor 1 (NE-DF) and Sensor 2 (NC-DD) shown in Figure 3.1 and draining into Grand Passage were not modelled.

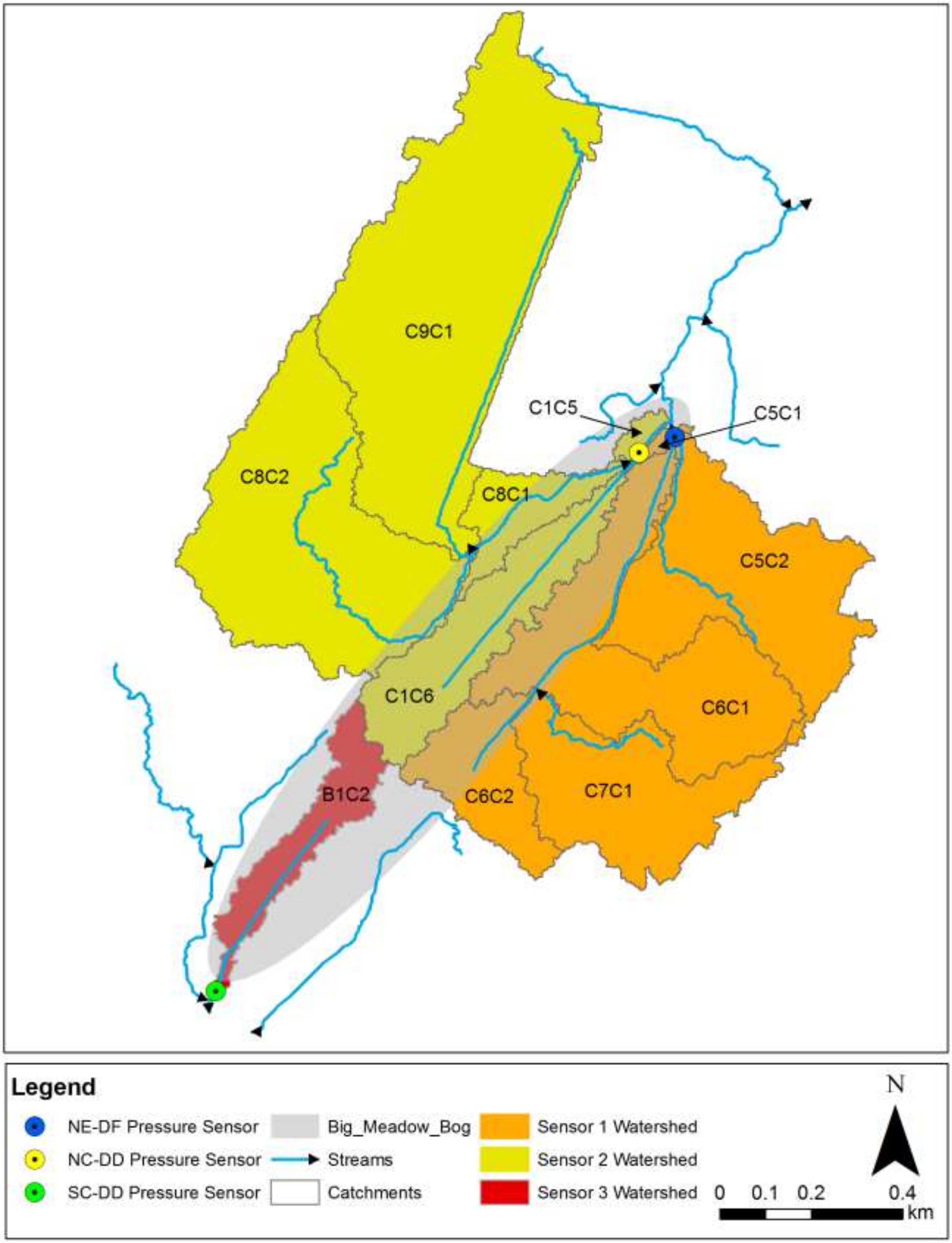

Figure 3.1: Catchments and watersheds for each of the three sensors.

The breakdown of overland flow, interflow, and base flow at each sensor location is presented below, in Table 3.1 for a typical low flow scenario, and for a high flow scenario such as the event on July 5, 2014 and shown in Figure 3.2 through Figure 3.4 for July, 2014. As expected, during times of low flow the only flow is base flow, with the exception of Sensor 1, which has some inter flow. Overland flow during the precipitation events is highest at Sensor 2 (NC-DD), and lowest at Sensor 3 (SC-DD), where the three peaks differ by an order of magnitude. Peaks in interflow lag the peaks in overland flow, marking the transition from overland flow to baseflow. The flows per catchments shown in Figure 3.2 through Figure 3.4 show how much each catchment is contributing to the total flow, which is based mainly on area. Overland, inter and base flows per catchment for each sensor between July 1 and Nov. 30 are presented in Appendix B.

	Sensor 1 NE-DF		**Sensor 2 NC-DD**		**Sensor 3 SC-DD**	
	Low Flow	**High Flow**	**Low Flow**	**High Flow**	**Low Flow**	**High Flow**
Overland Flow	0	2×10^{-1}	0	1	0	5×10^{-2}
Inter Flow	1×10^{-3}	4×10^{-3}	0	6×10^{-3}	0	5×10^{-4}
Base Flow	$\sim 1.8 \times 10^{-3}$	2×10^{-3}	Declines from 0.09 to 0.05		Declines from 0.01^{2} to 0.006	

Table 3.1: All flows in m^3/s. Breakdown of overland, inter, and base flow for each sensor (watershed) during low flow periods, and during a high flow (high precipitation) event such as the one on July 5, 2014.

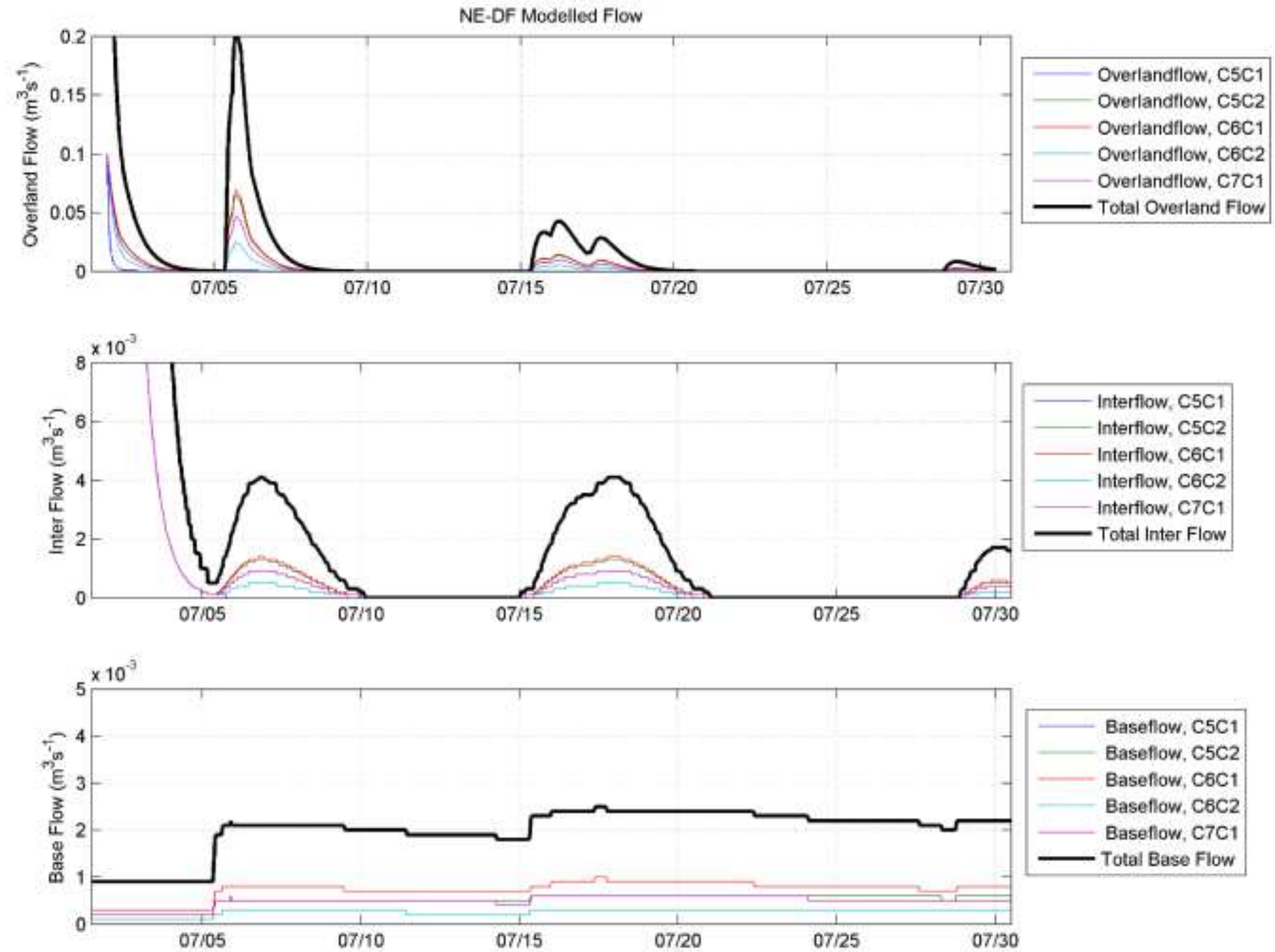

Figure 3.2: Modelled overland, inter, and base flow for the NE-DF during July 2014.

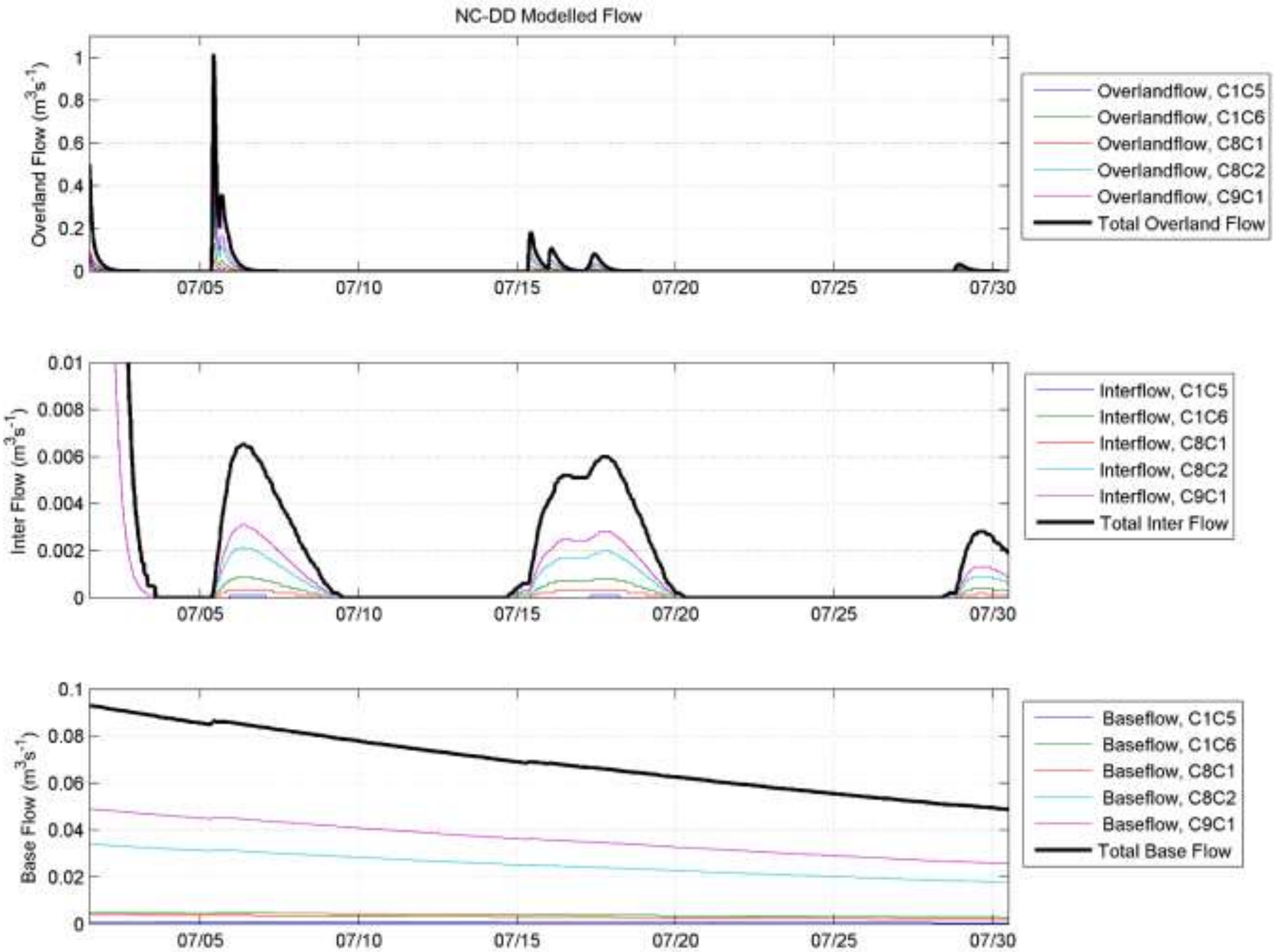

Figure 3.3: Modelled overland, inter, and base flow for the NC-DD during July 2014.

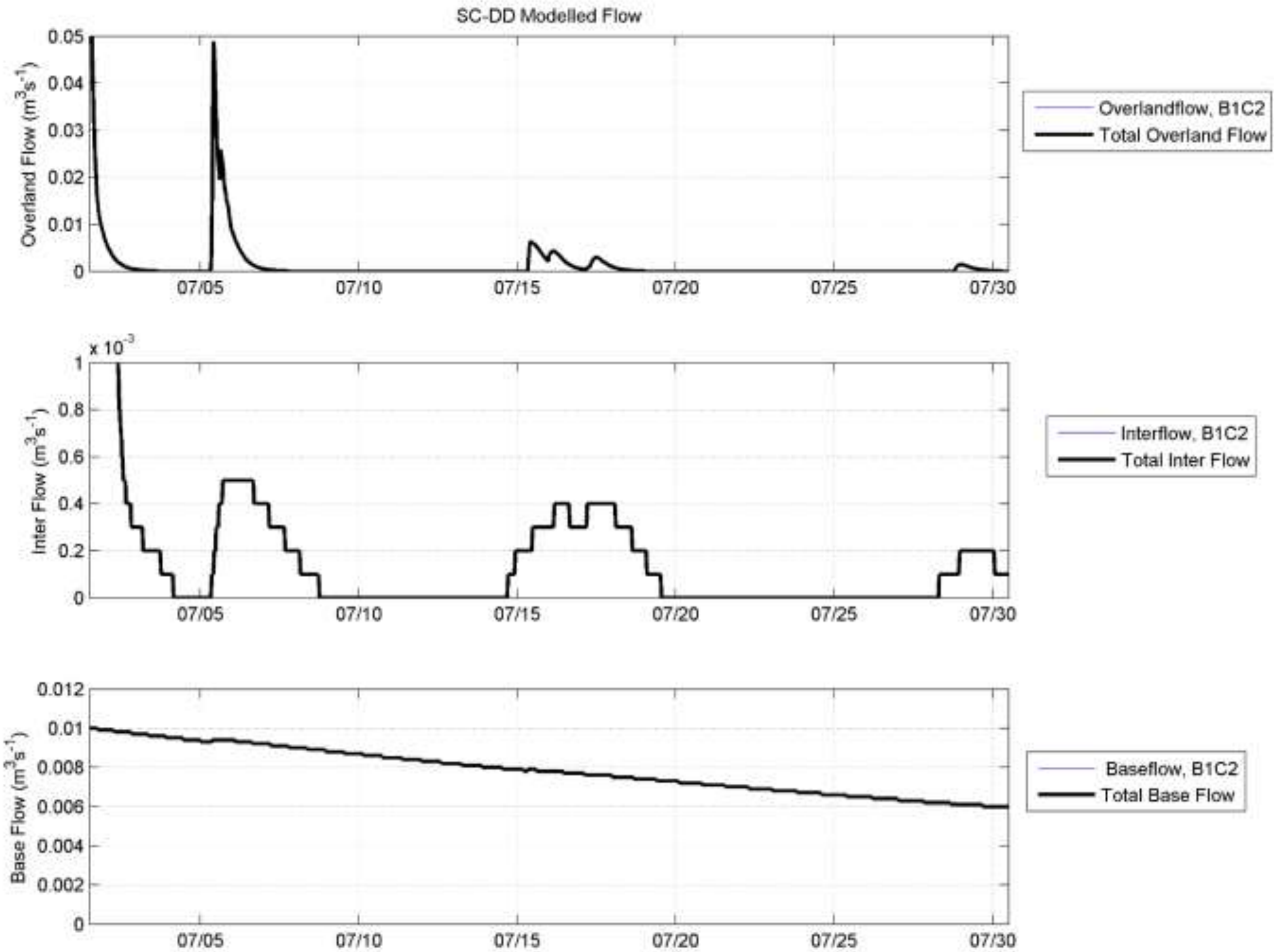

Figure 3.4: Modelled overland, inter, and base flow for the SC-DD during July 2014.

We can also examine the breakdown of flow at each sensor by percent (Figure 3.5 and Figure 7.5). We again see that overland flow dominates during precipitation events at all three sensor locations, and we see that base flow makes up the entire flow during dry periods. At Sensor 1, the transition from an overland flow-dominated system to a base flow dominated system is longer than at Sensors 2 and 3 (the sensors on the drainage ditch), which is consistent with the water level observations and modelled discharge (Figure 2.18). This implies that the NE-DF is behaving more like a typical river, and rainfall that arrives in the stream during and following a rainfall event slowly drains through the stream network, exiting the system into Grand Passage; whereas at the sensors along the artificial drainage ditch, water entering the ditch is quickly absorbed by the bog and flow returns to base-flow-dominated more quickly. While Figure 3.5 shows July only, Figure 7.5 shows July 1 – November 30, showing how the breakdown of flow is different at the three sensors during different levels of precipitation events. During small rainfall events in August the overland flow does not make up 100% of the total flow as it does during larger precipitation events.

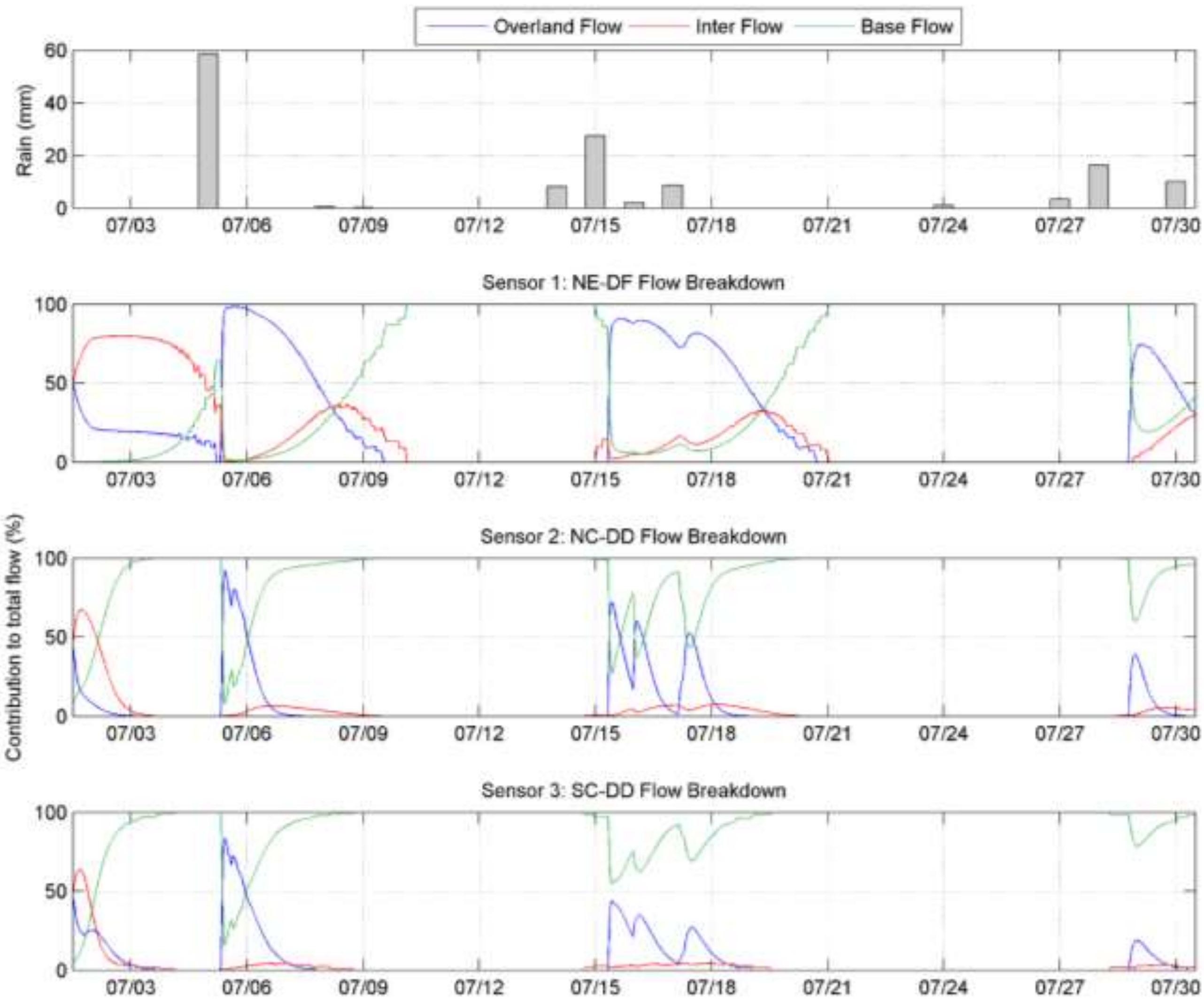

Figure 3.5: Contribution of overland, inter and base flow to total flow at each sensor location during July 2014.

3.2 Outlet Ranking

In order to better understand how each catchment was contributing to the runoff at the sensor locations, each stream branch (outlet) was ranked by runoff and by area (Table 3.2). For this analysis, we have considered the Oct 20 – Nov 30 simulation (Figure 2.17) because it represents wet conditions and good model performance (sustained baseflow). In general, the rankings by runoff and by area agree, such that larger catchment areas have larger total runoff. These results are sensible, as model inputs and initial baseflow values are all normalized by area. Any ranking of ungauged and uncalibrated streams outside the modelled watersheds would be based on assumptions of similarities with other streams, therefore that analysis is not presented here.

Catchment Name	Catchment Area (km^2)	Total Runoff Oct 20- Nov 30	Rank by Runoff	Rank by Area
C9C1	0.358	113.2756	1	1
C8C2	0.251	79.6945	2	2
C6C1	0.185	31.8921	3	3
C5C2	0.174	29.8127	4	4
C7C1	0.125	23.2777	5	5
C1C6	0.103	23.0358	6	6
B1C2	0.056	22.6516	7	8
C6C2	0.066	14.6675	8	7
C8C1	0.041	13.0515	9	9
C5C1	0.003	4.9374	10	11
C1C5	0.007	4.5301	11	10

Table 3.2: Areas, total flows between October 20 and November 30, ranked by runoff and rank by area for each modelled catchment.

4 Discussion and Limitations

Hydrodynamic modelling of the Brier Island Big Meadow Bog drainage features and ditches presented some unique challenges, beginning with the rating curves. The observed flow data, cross-sectional measurements, and measured water levels did not produce suitable rating curves. This is likely related to the physical nature of the drainage features and ditches themselves: soft sediement, dynamic banks, and the narrow widths of the channels all contributed to difficulty in obtaining precise and consistent measurements. Secondly, the central drainage ditch did not flow in a manner typical of overland flow, bur rather more like the bog drainage features that they are, but unfortunately means that rating curves are not a suitable way to convert water level to discharge. The lack of rating curves was not unsurmountable, but meant that we bypassed the usual step of calibrating the river runoff model outside of the hydrodynamic model, which added complexity to the system.

We were successful in modelling the NE-DF (Sensor 1) using the Mike 1-D model, but the central drainage ditch was more of a challenge. Ultimately, we were not able to change model parameters to cause baseflow to recharge properly over long simulations; however, model performance over short simulations (~ 1 month) was suitable and we feel that the results from the short simulations are accurate representations of the bog.

The study could be improved by adding additional water level gauges, or even additional rain sensors farther south in the watershed.

5 References

DHI, 1999 http://iwmi.dhigroup.com/hydrological_cycle/streamflow.html

MacDonald and Webster, 2014. Brier Island Hydrological Analysis. Report to Nature Conservancy of Canada, 32 pp.

MacDonald and Webster, 2015. Classification of Multispectral Aerial Photography of Big Meadow Bog on Brier Island, Nova Scotia. Report to Nature Conservancy of Canada, 49 pp.

http://www.fsl.orst.edu/geowater/FX3/help/8_Hydraulic_Reference/Mannings_n_Tables.htm

6 Appendix A: Weather Plots

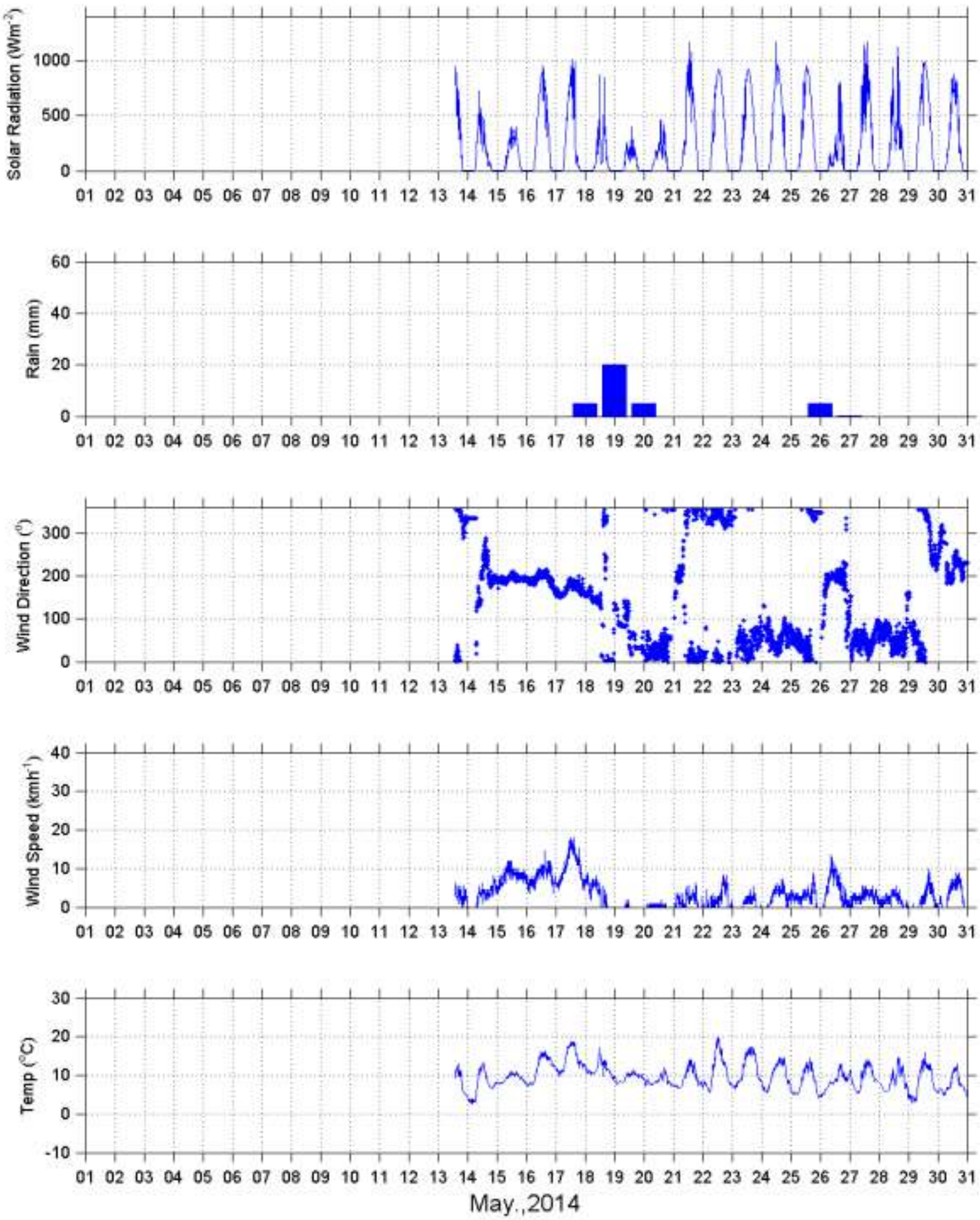

Figure 6.1: AGRG Weather station data for May 2014.

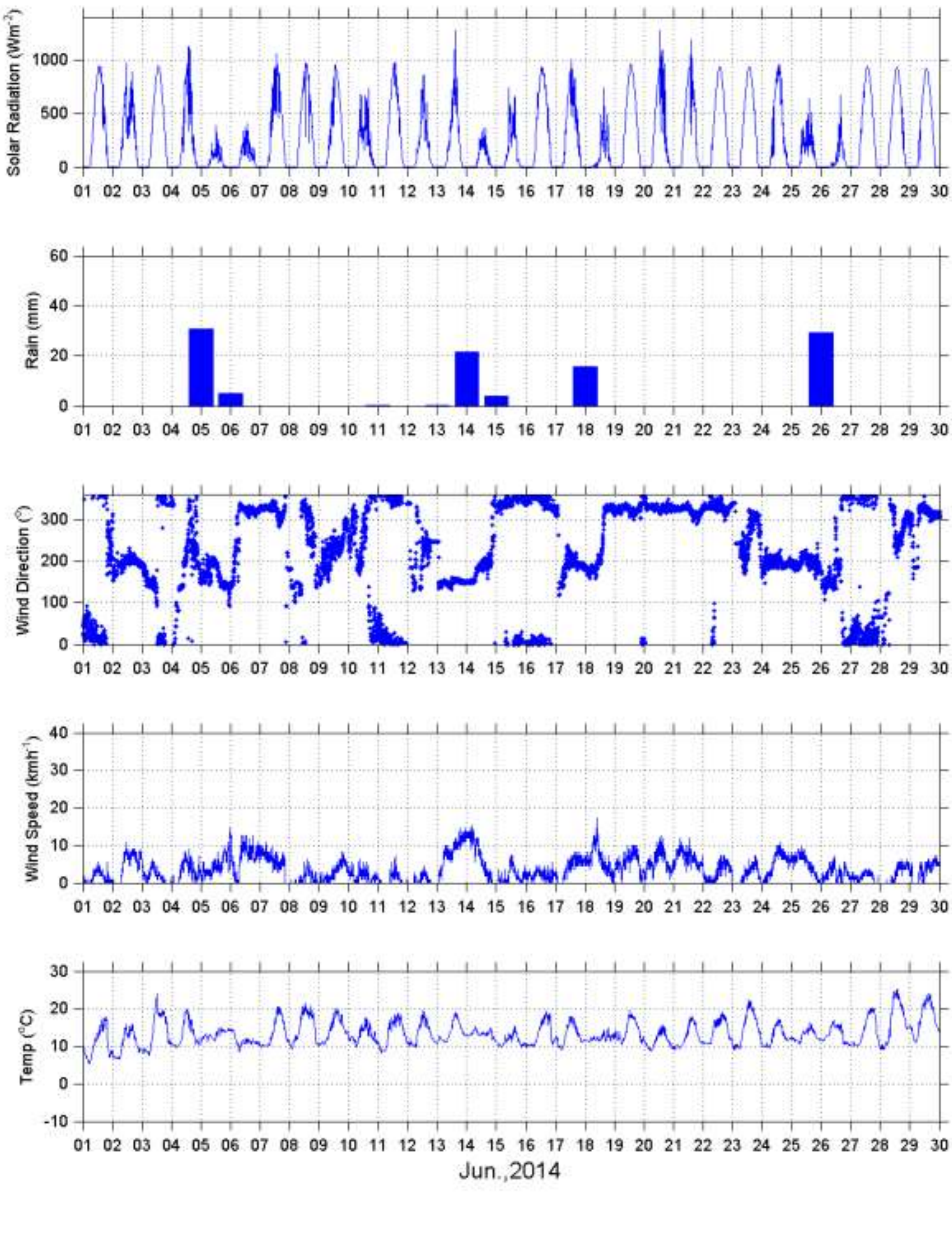

Figure 6.2: AGRG Weather station data for June 2014.

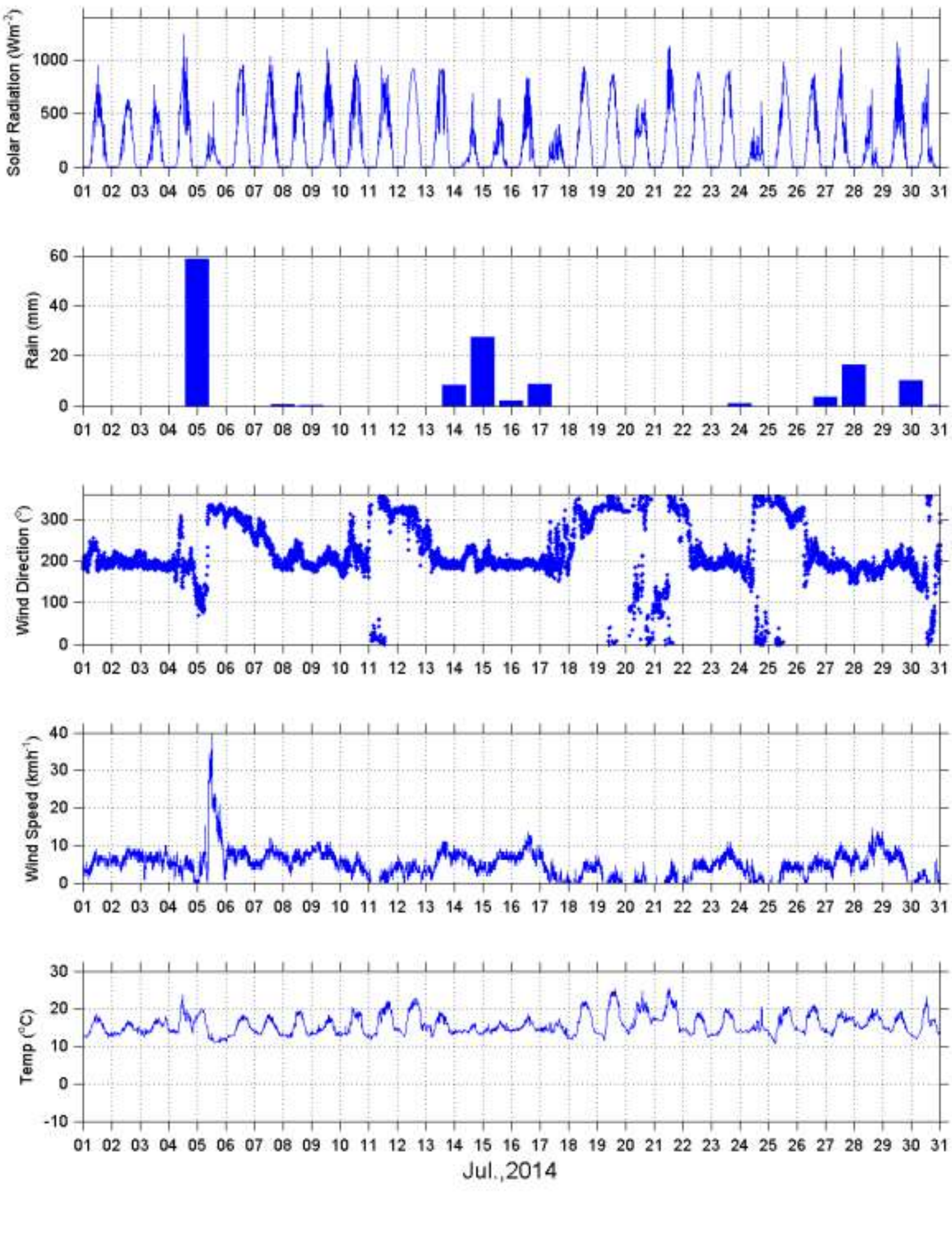

Figure 6.3: AGRG Weather station data for July 2014.

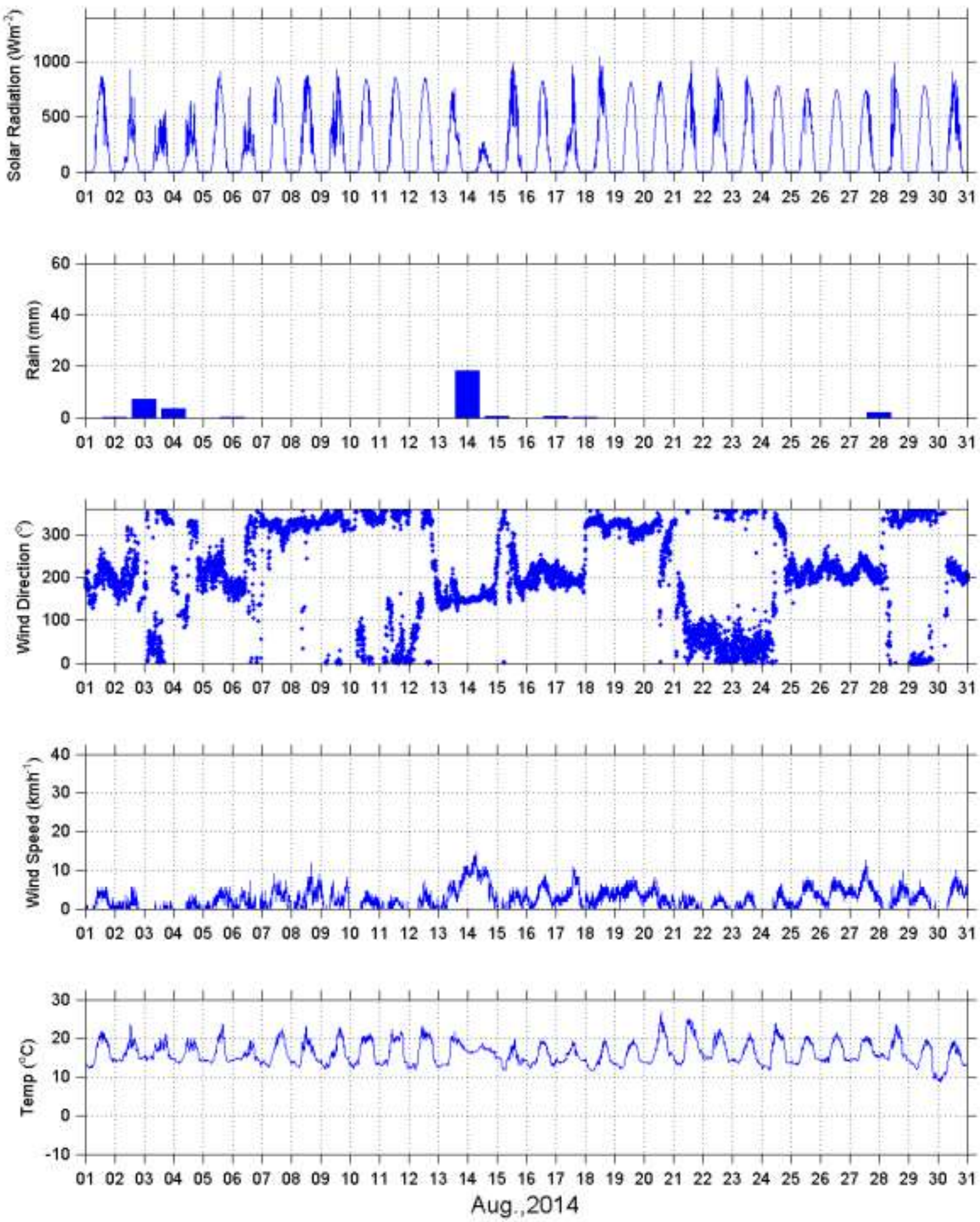

Figure 6.4: AGRG Weather station data for August 2014.

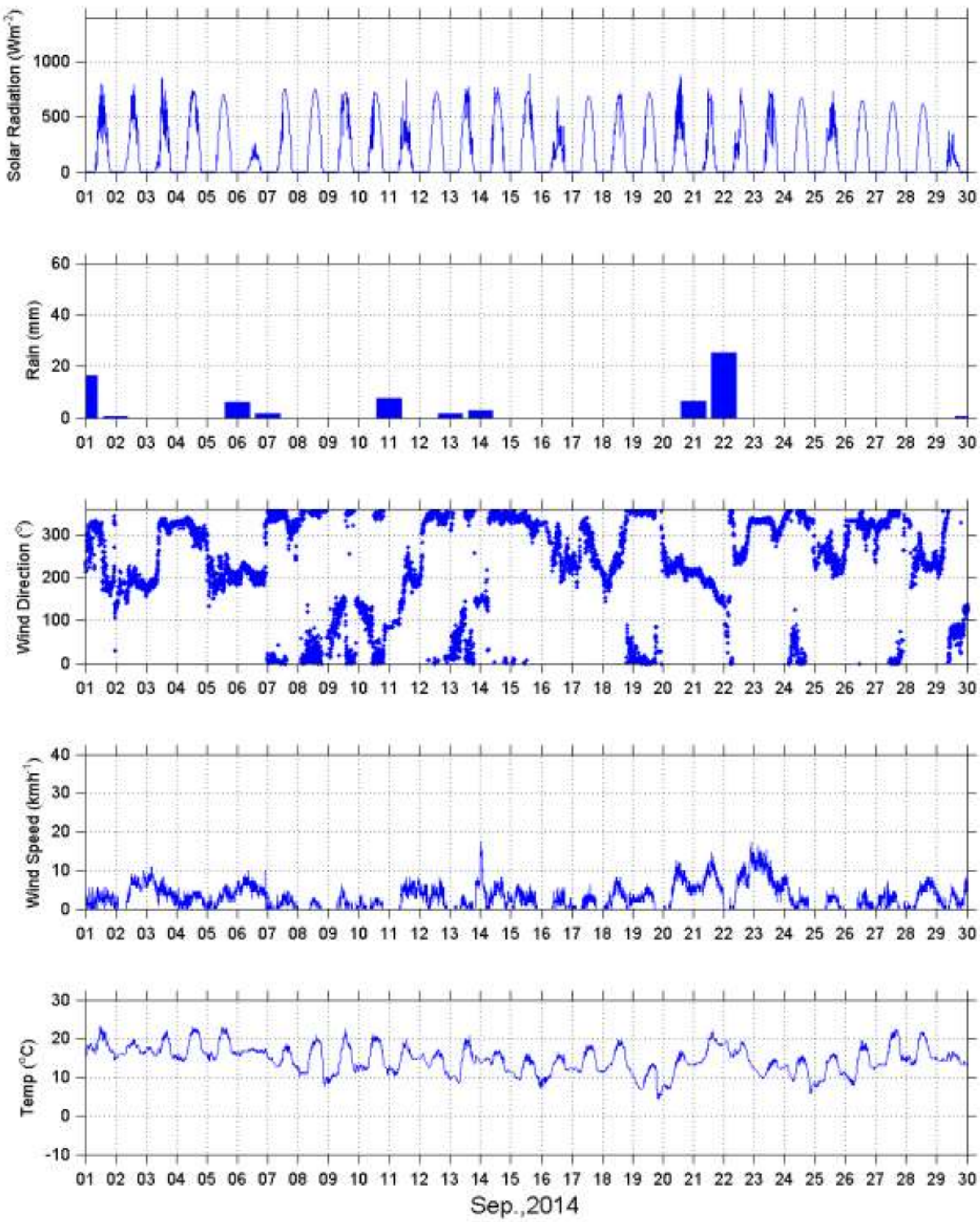

Figure 6.5: AGRG Weather station data for September 2014.

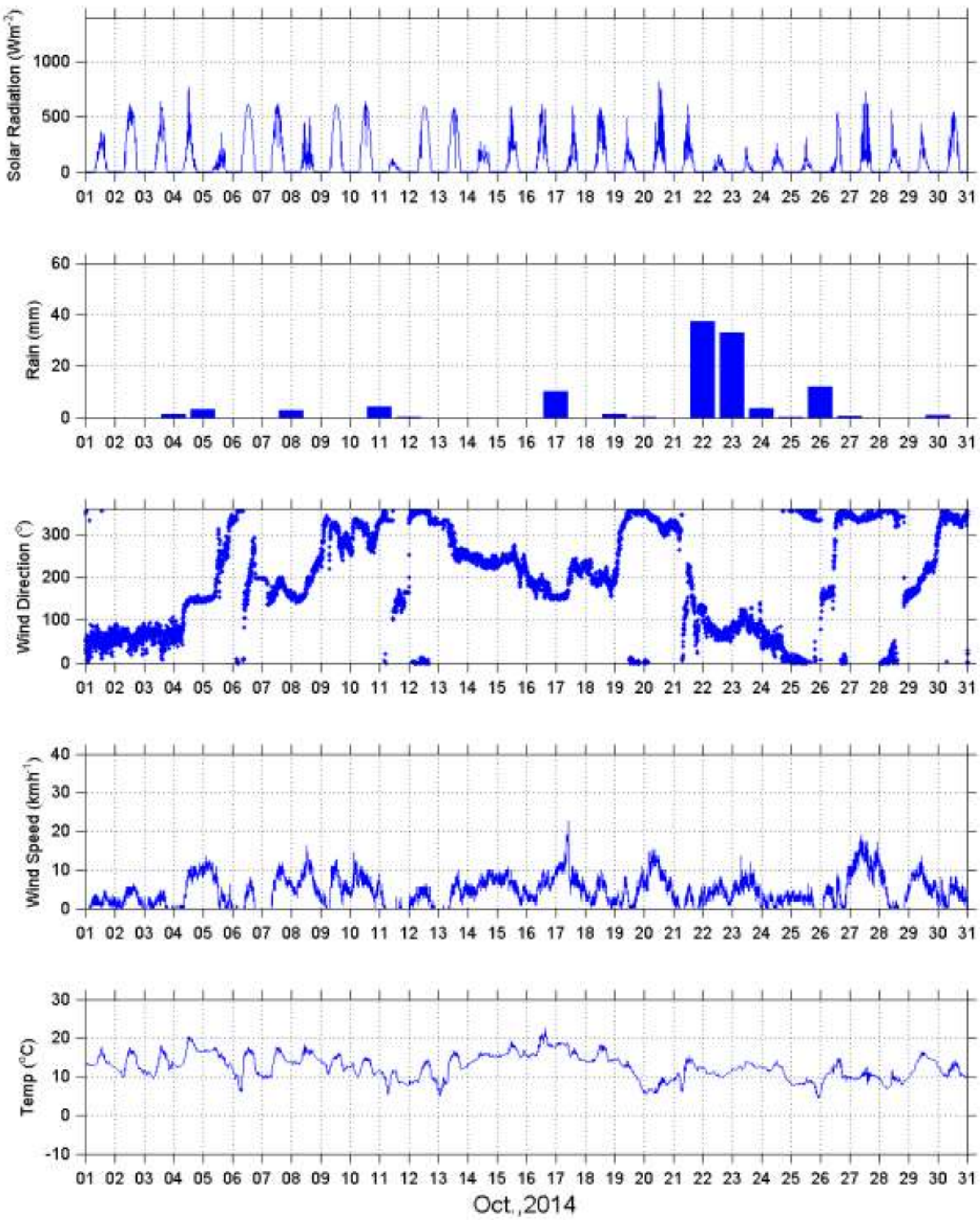

Figure 6.6: AGRG Weather station data for October 2014.

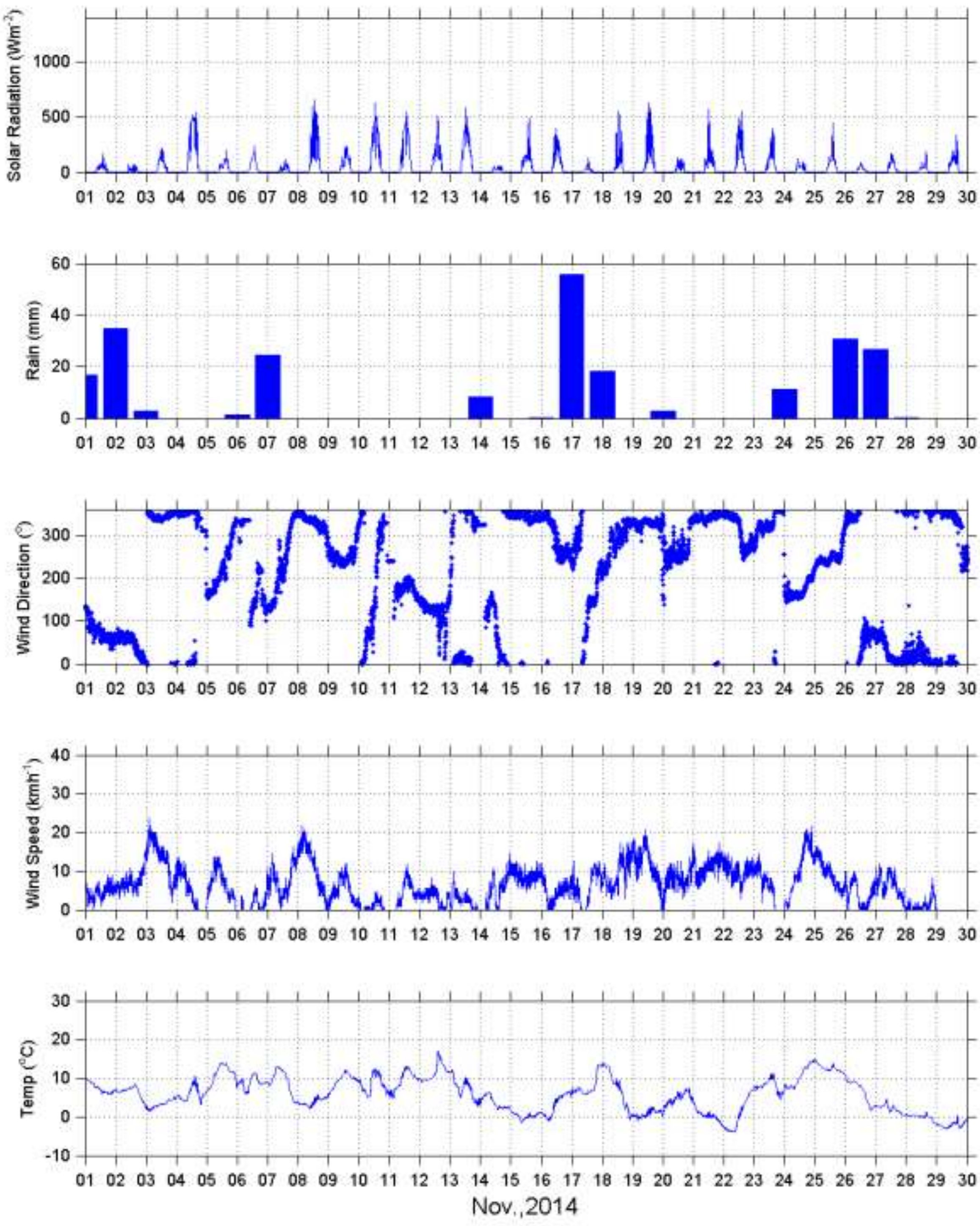

Figure 6.7: AGRG Weather station data for November 2014.

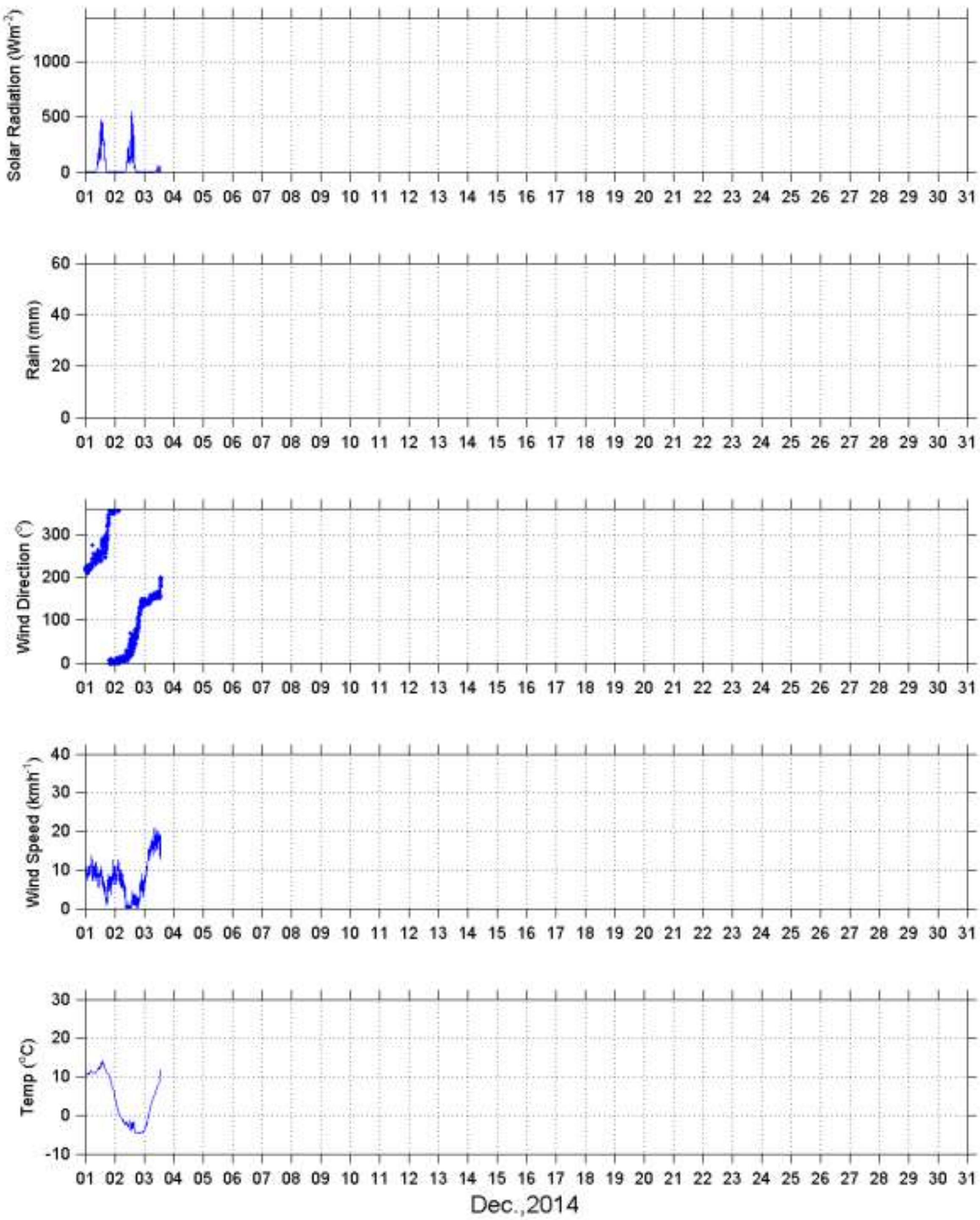

Figure 6.8: AGRG Weather station data for December 2014.

7 Appendix B: Extra Figures

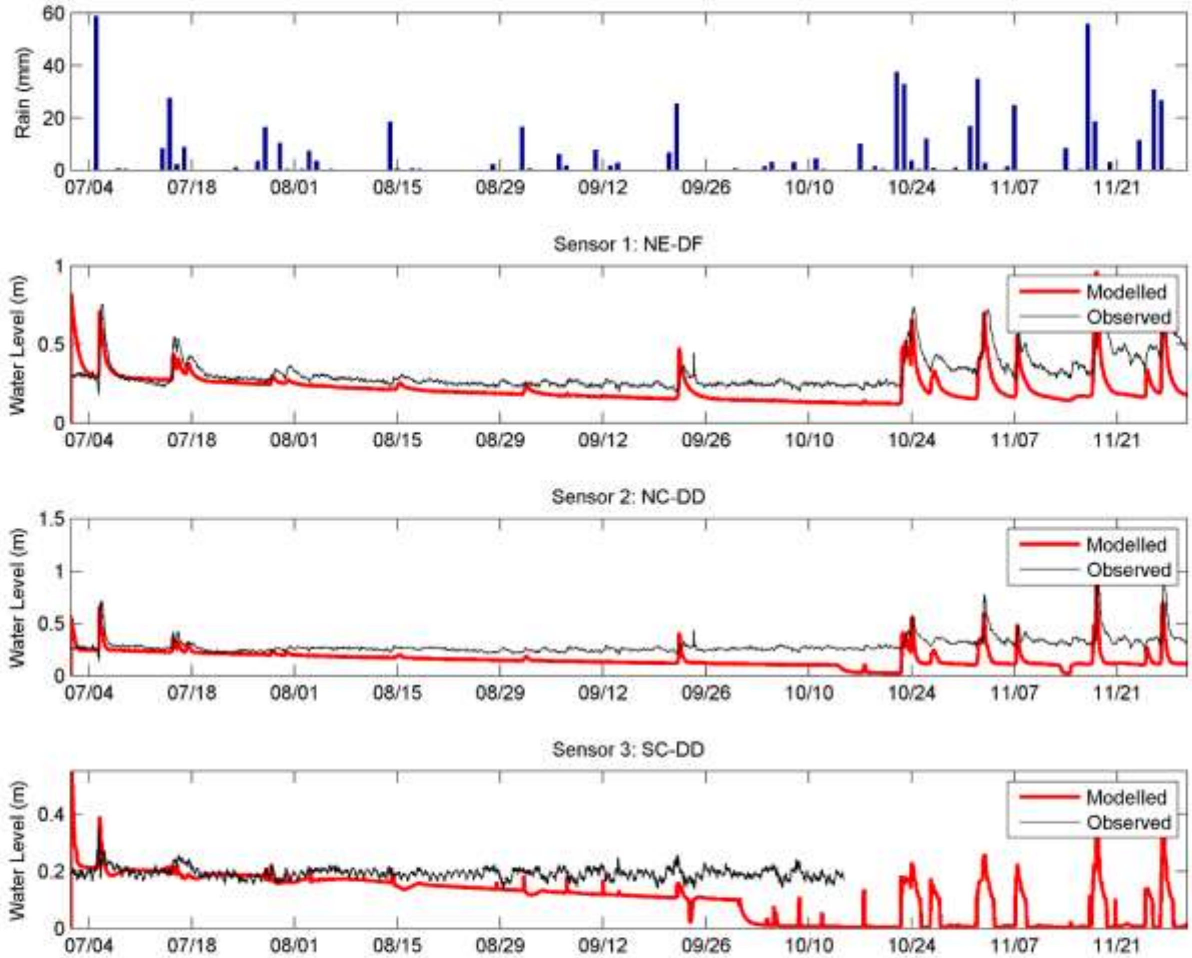

Figure 7.1: Water level calibration plot for July 1 – Nov. 30, 2014.

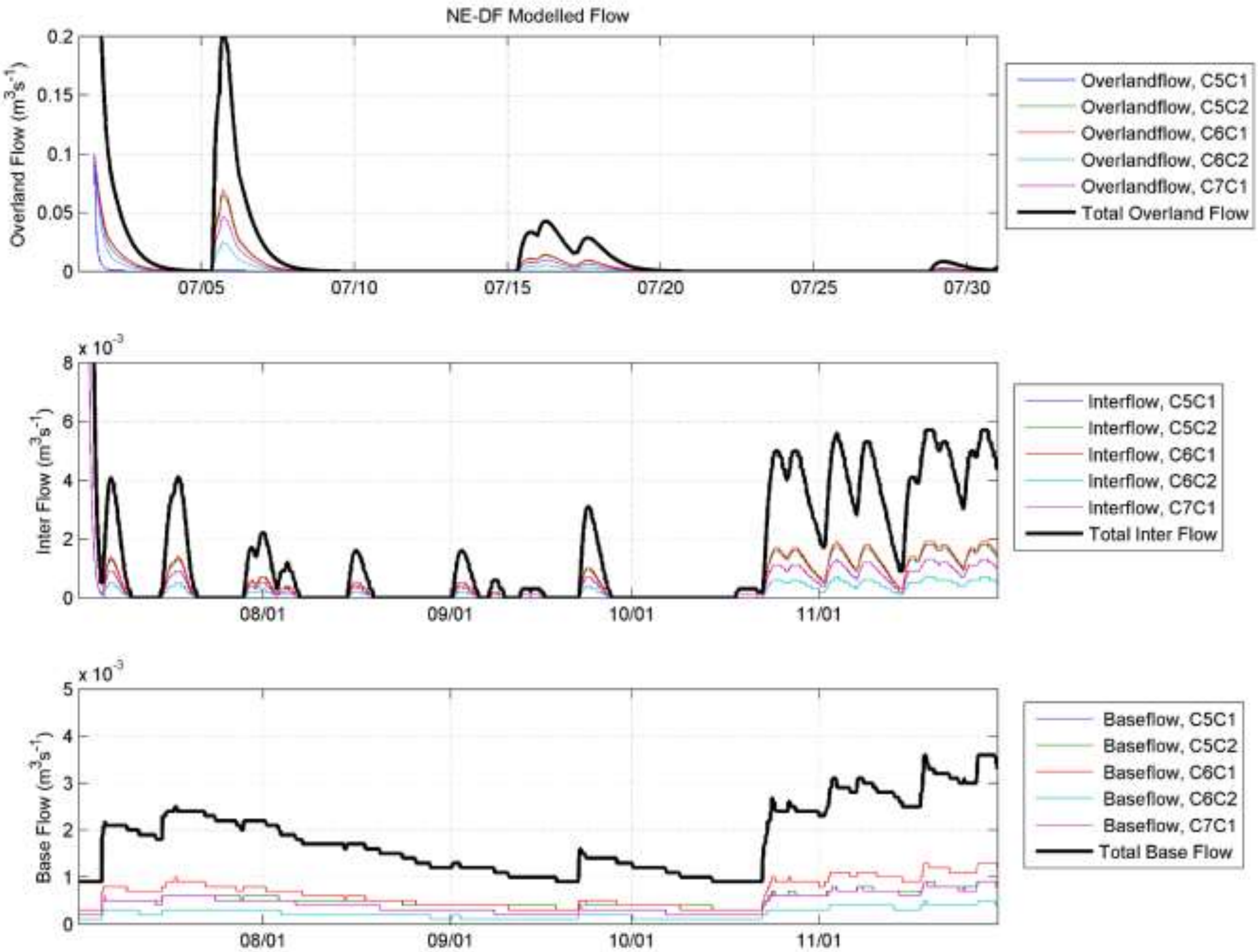

Figure 7.2: Modelled overland, inter, and base flow for the NE-DF between July 1 and November 30, 2014.

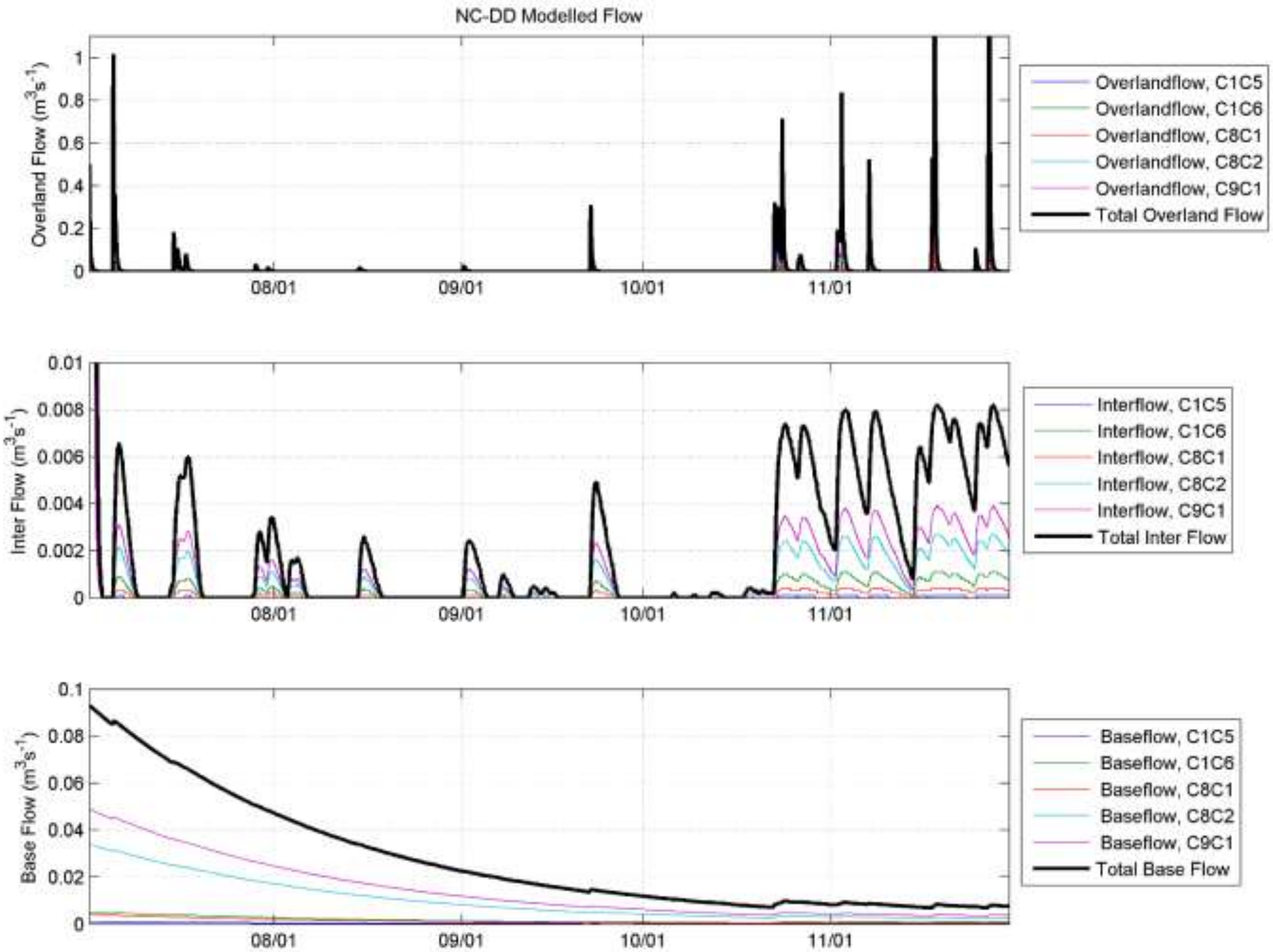

Figure 7.3 Modelled overland, inter, and base flow for the NC-DD between May 15 and November 30, 2014.

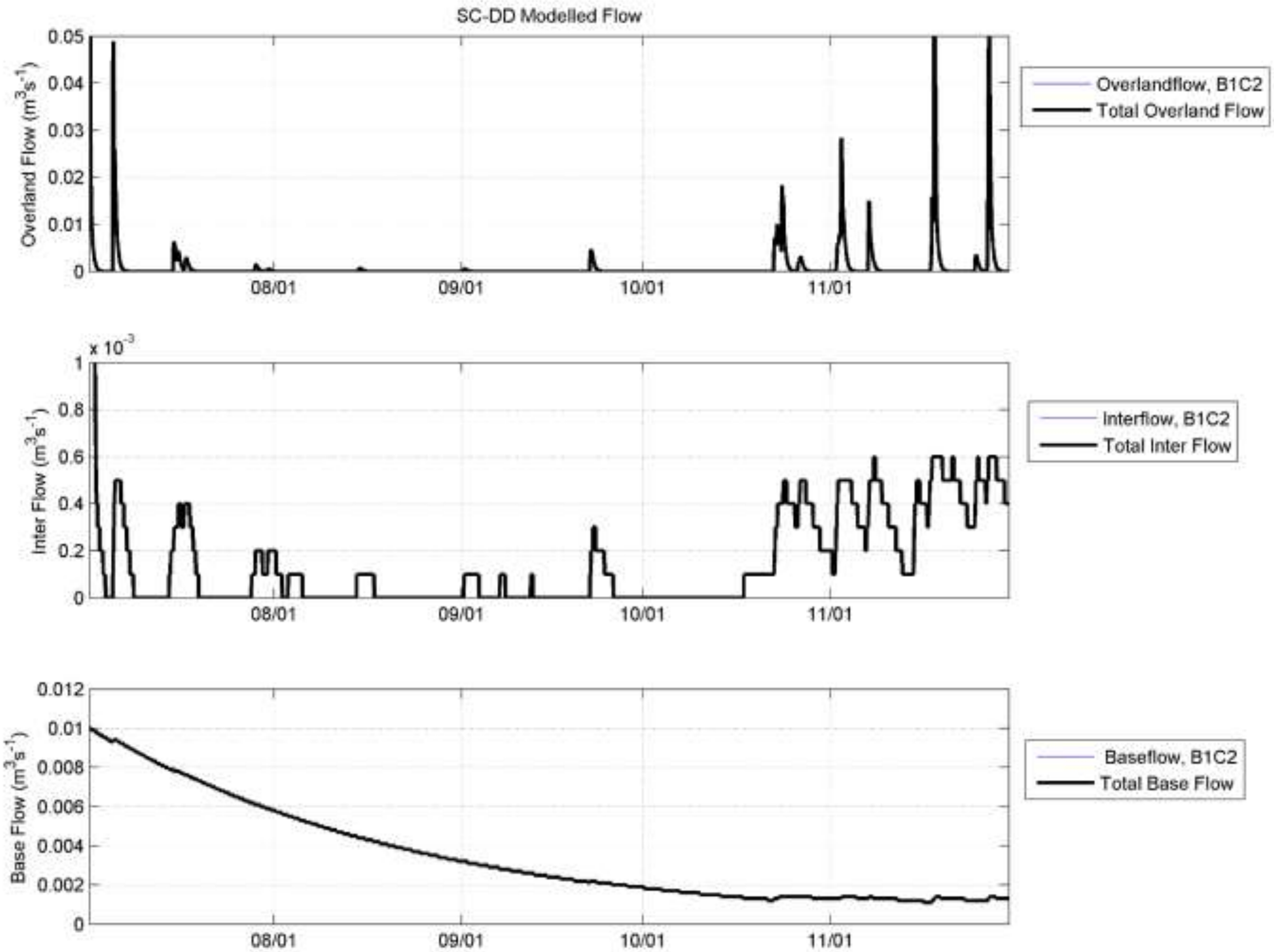

Figure 7.4: Modelled overland, inter, and base flow for the SC-DD between May 15 and November 30, 2014.

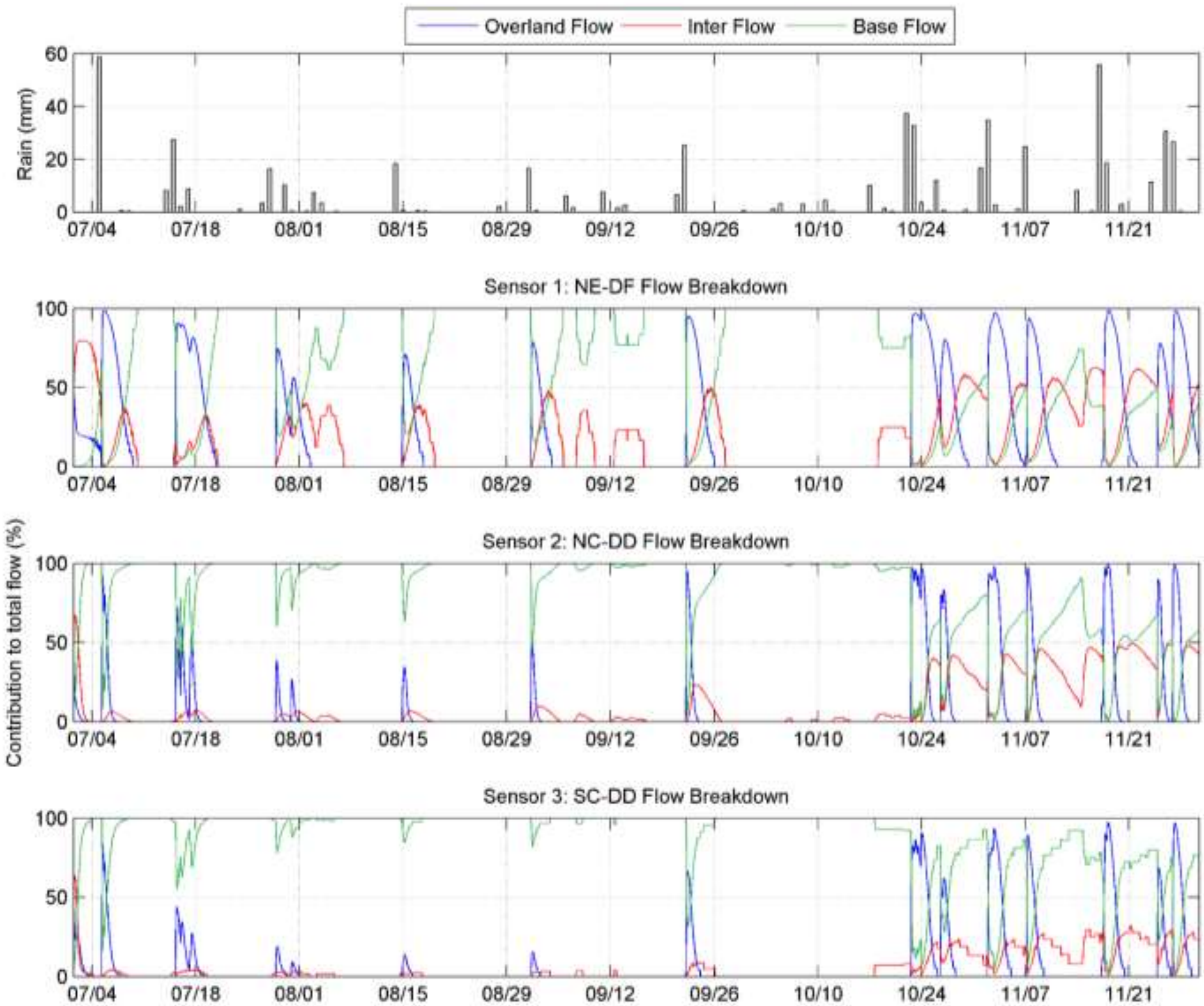

Figure 7.5: Contribution of overland, inter and base flow to total flow at each sensor location between May 15 and Nov. 30, 2014.